Laser Pulse Control of Ultrafast Transfer Processes in Molecular Nanostructures

Volkhard May, Institute of Physics
Humboldt-University at Berlin

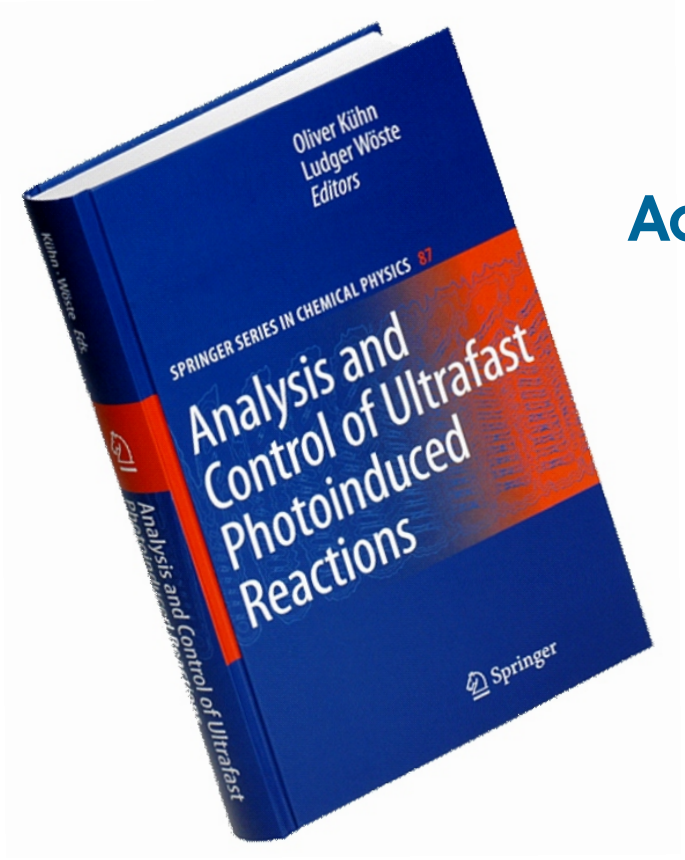

Acknowledgment:
T. Mancal
B. Brüggemann
A. Kaiser
L. Wang
DFG (Sfb 450)

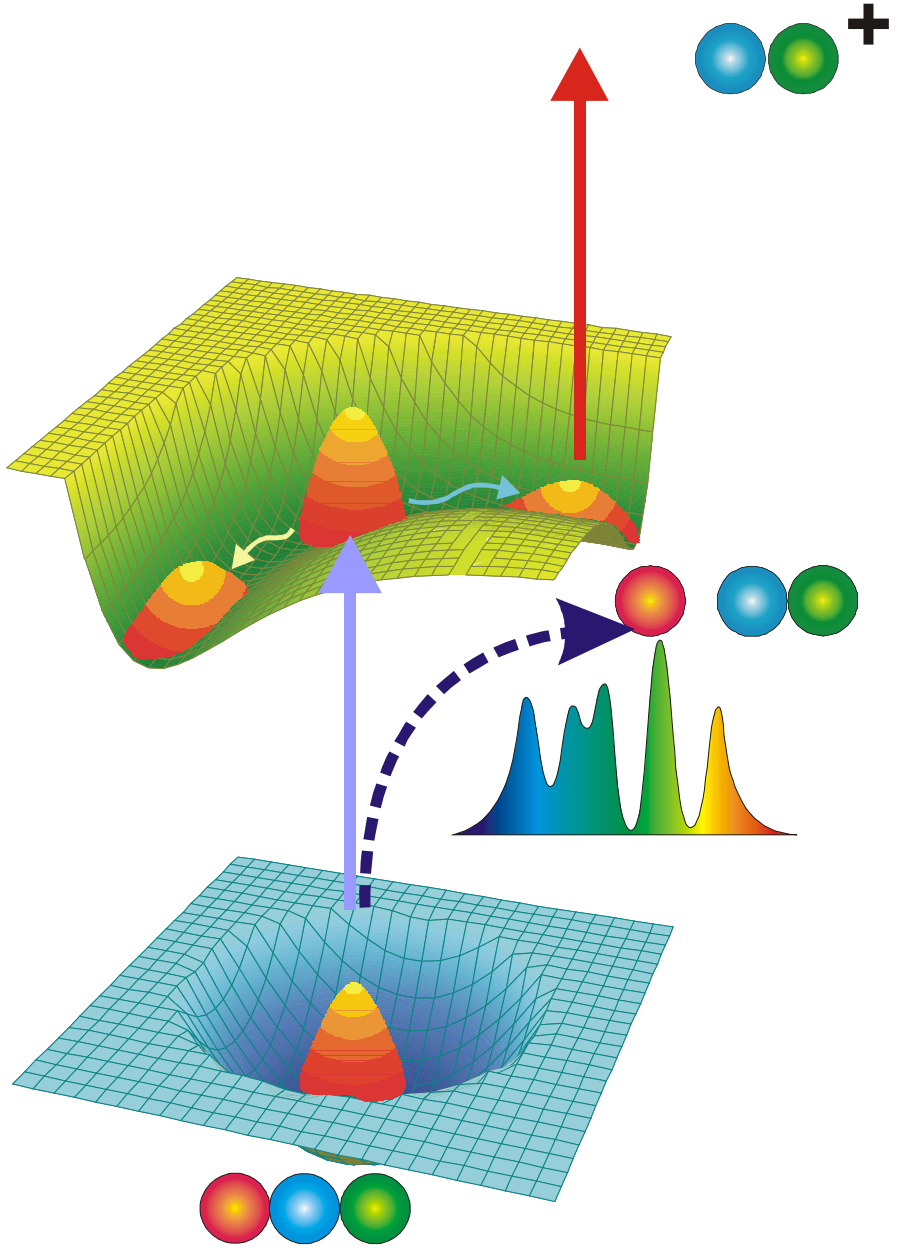

Experiment

Adaptive Femtosecond Quantum Control

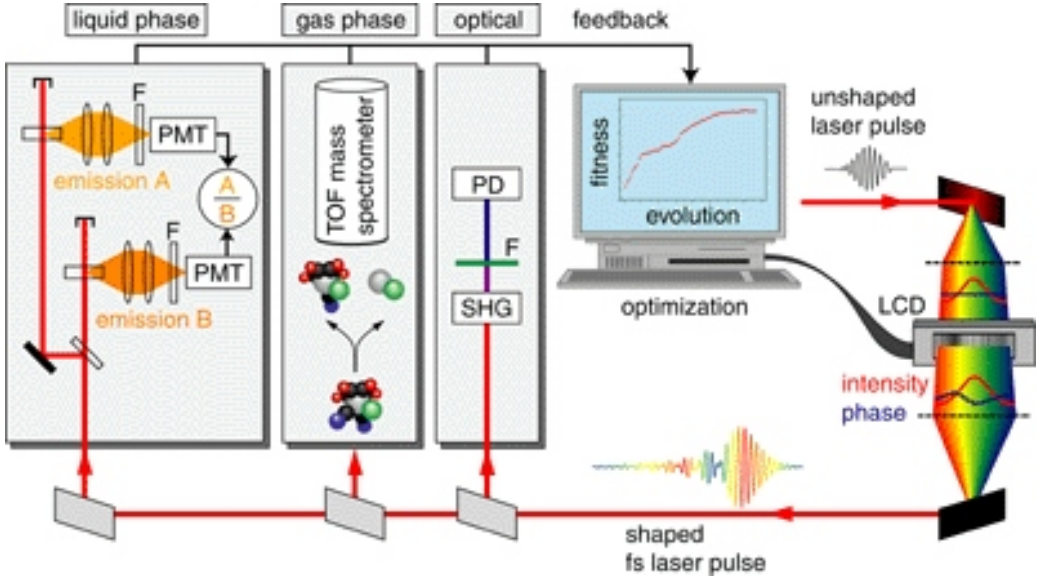

G. Gerber

Theory

Optimal Control Theory

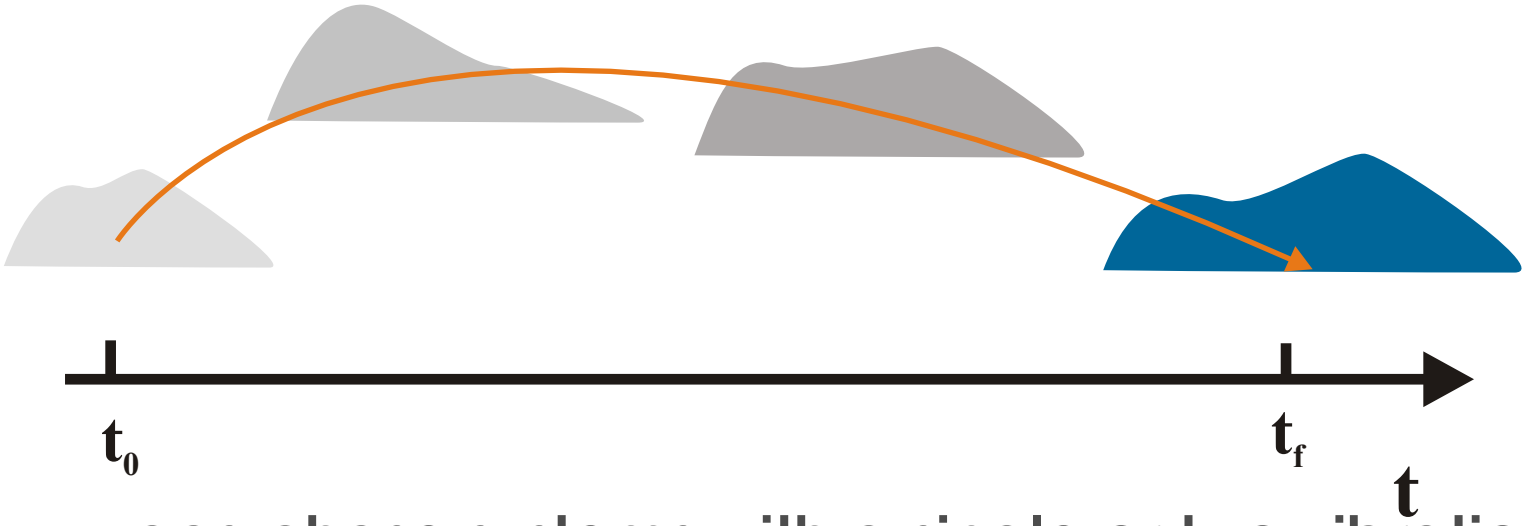

- gas-phase systems with a single or two vibrational DOF
- account for laser field fluctuations and intensity profile

- a single DOF coupled to a heath bath
- random orientation
- static disorder
- optimization of an observable
- control of particle motion

A Simple Example

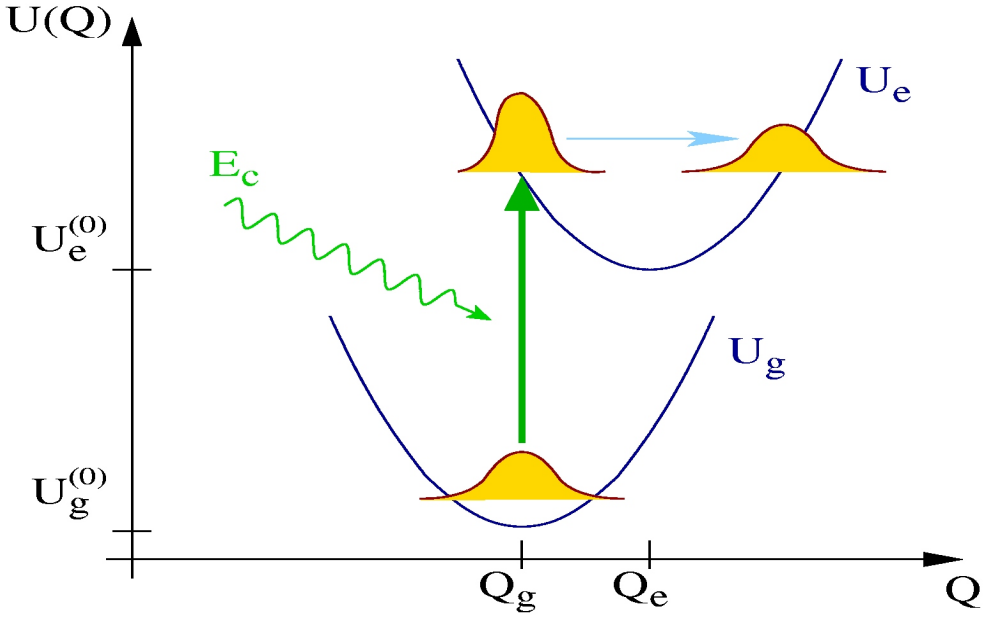

Two level model with harmonic PES.

- **Initial state:**

$$|\psi_0\rangle = |\phi_g\rangle\,|\chi_{g,0}\rangle$$

- **Target state:**

$$|\psi_{\text{tar}}\rangle = |\phi_e\rangle\,|\chi_{\text{tar}}\rangle$$

- **Target time:**

$$t_f = 100 \text{ fs}$$

- $J_0[\mathbf{E}_c] = |\langle\psi_{\text{tar}}|\psi(t_f)\rangle|^2$

Zeroth iteration:

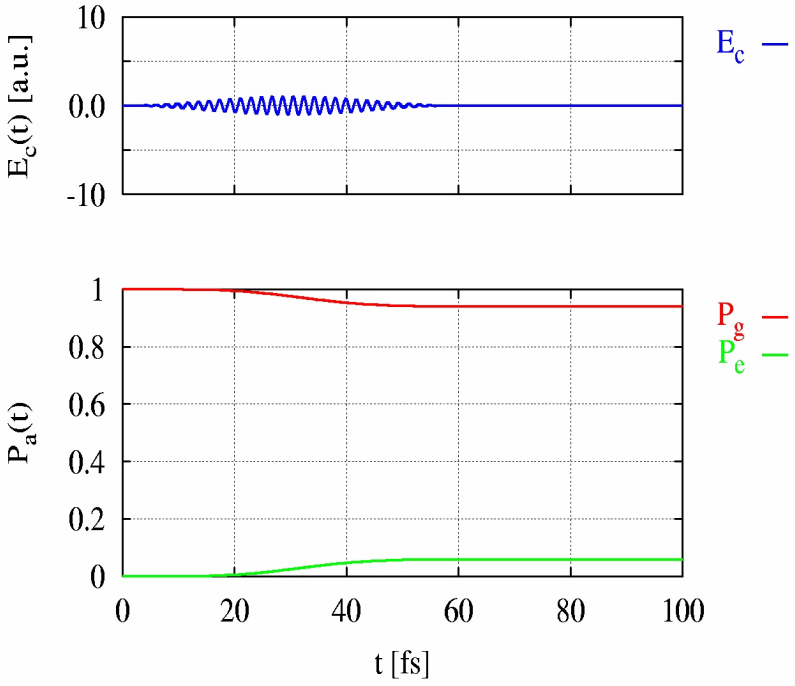

Control field (upper panel) and state population (lower panel).

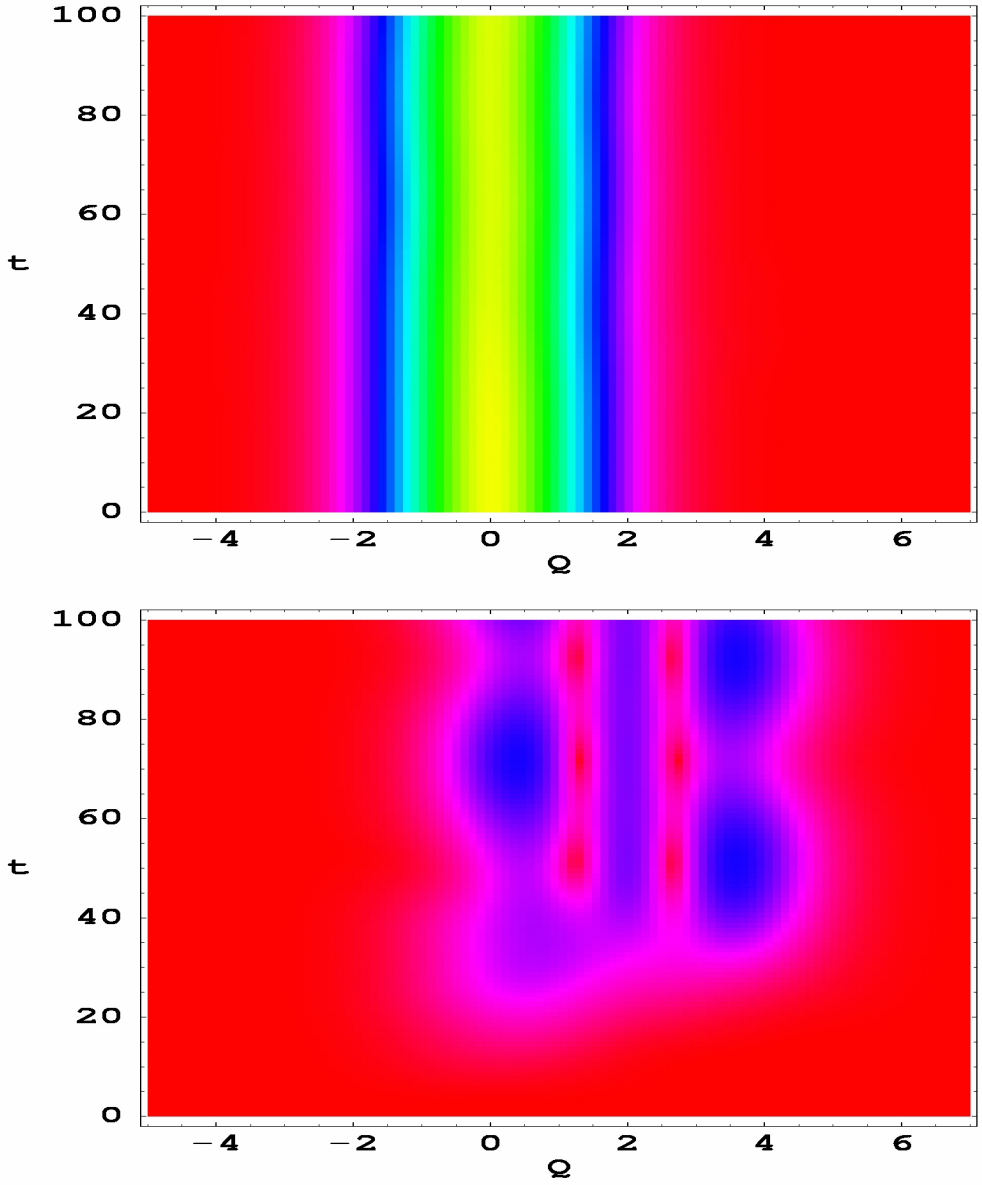

Vibrational wavepacket, ground state (upper panel), excited state (lower panel).

- Control yield

$$J_0^{(0)} = |\langle \psi_{\text{tar}} | \psi^{(0)}(t_f) \rangle|^2 = 0.02.$$

First iteration:

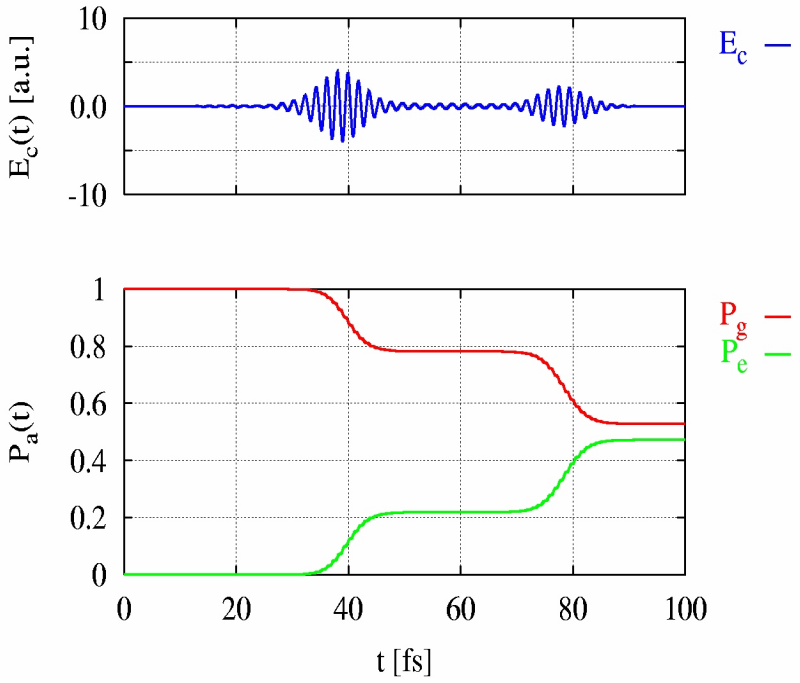

Control field (upper panel) and
state population (lower panel).

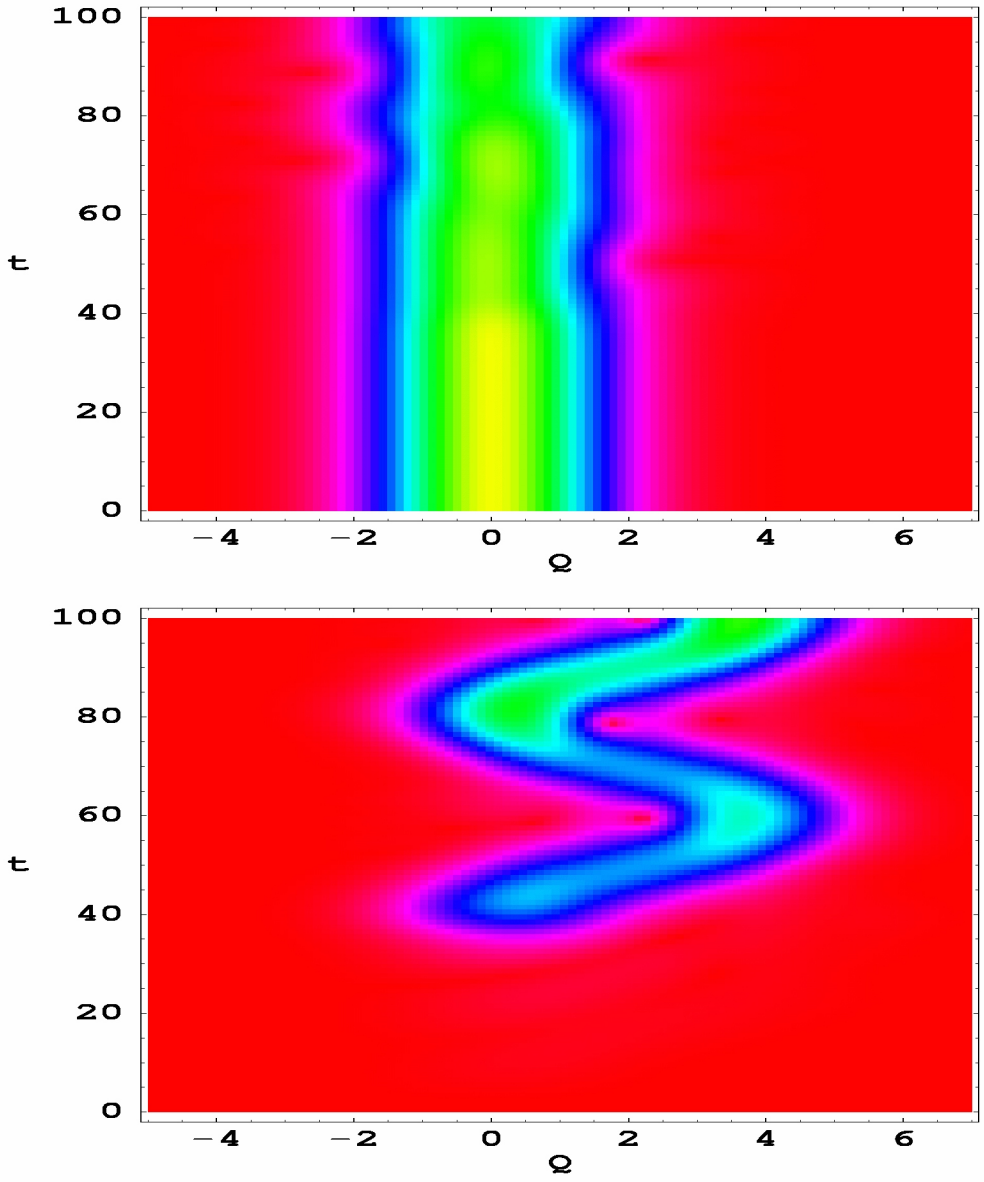

Vibrational wavepacket, ground state (upper panel),
excited state (lower panel).

- Control yield

$$J_0^{(1)} = |\langle \psi_{\text{tar}} | \psi^{(1)}(t_f) \rangle|^2 = 0.43.$$

Third iteration:

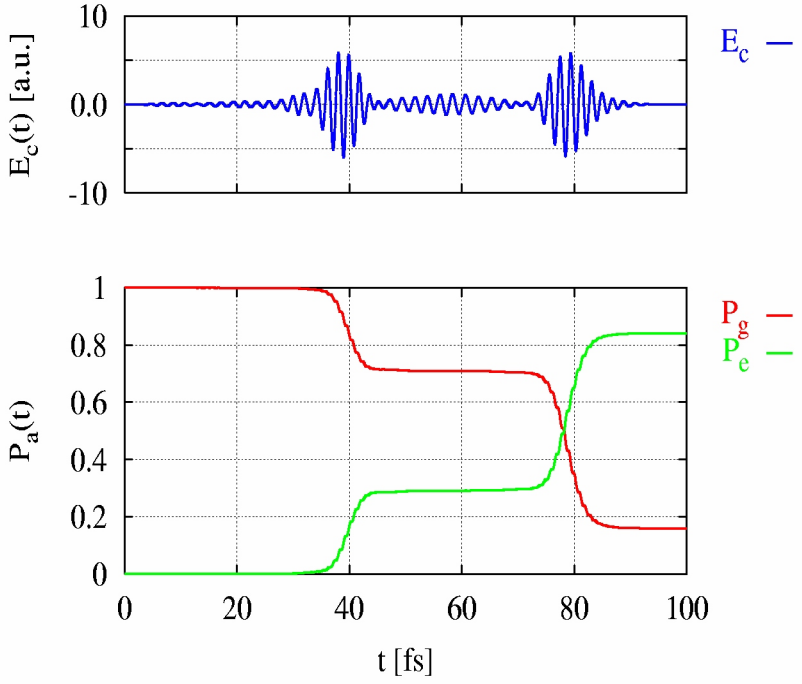

Control field (upper panel) and
state population (lower panel).

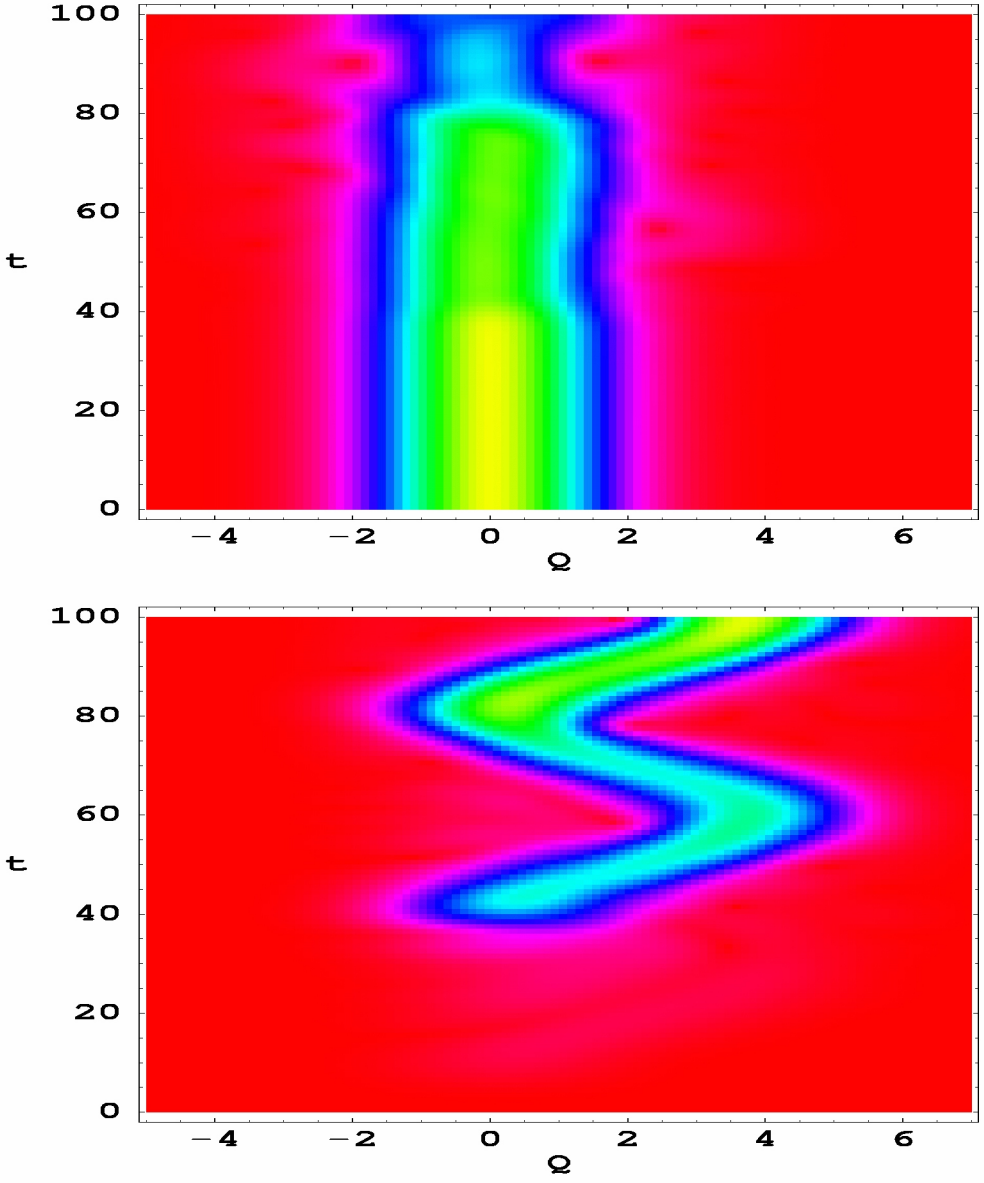

Vibrational wavepacket, ground state (upper panel),
excited state (lower panel).

- Control yield

$$J_0^{(3)} = |\langle \psi_{\text{tar}} | \psi^{(3)}(t_f) \rangle|^2 = 0.81.$$

20th iteration:

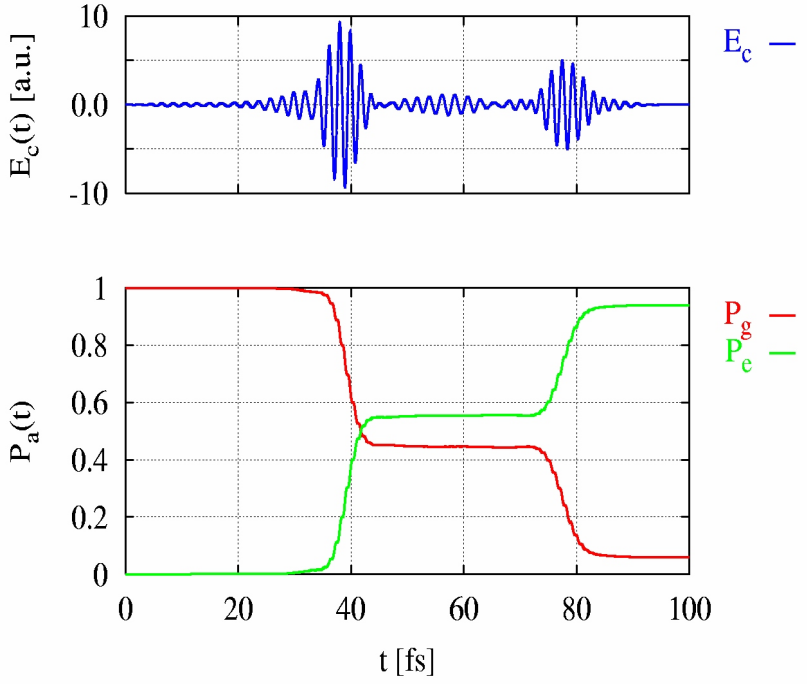

Control field (upper panel) and
state population (lower panel).

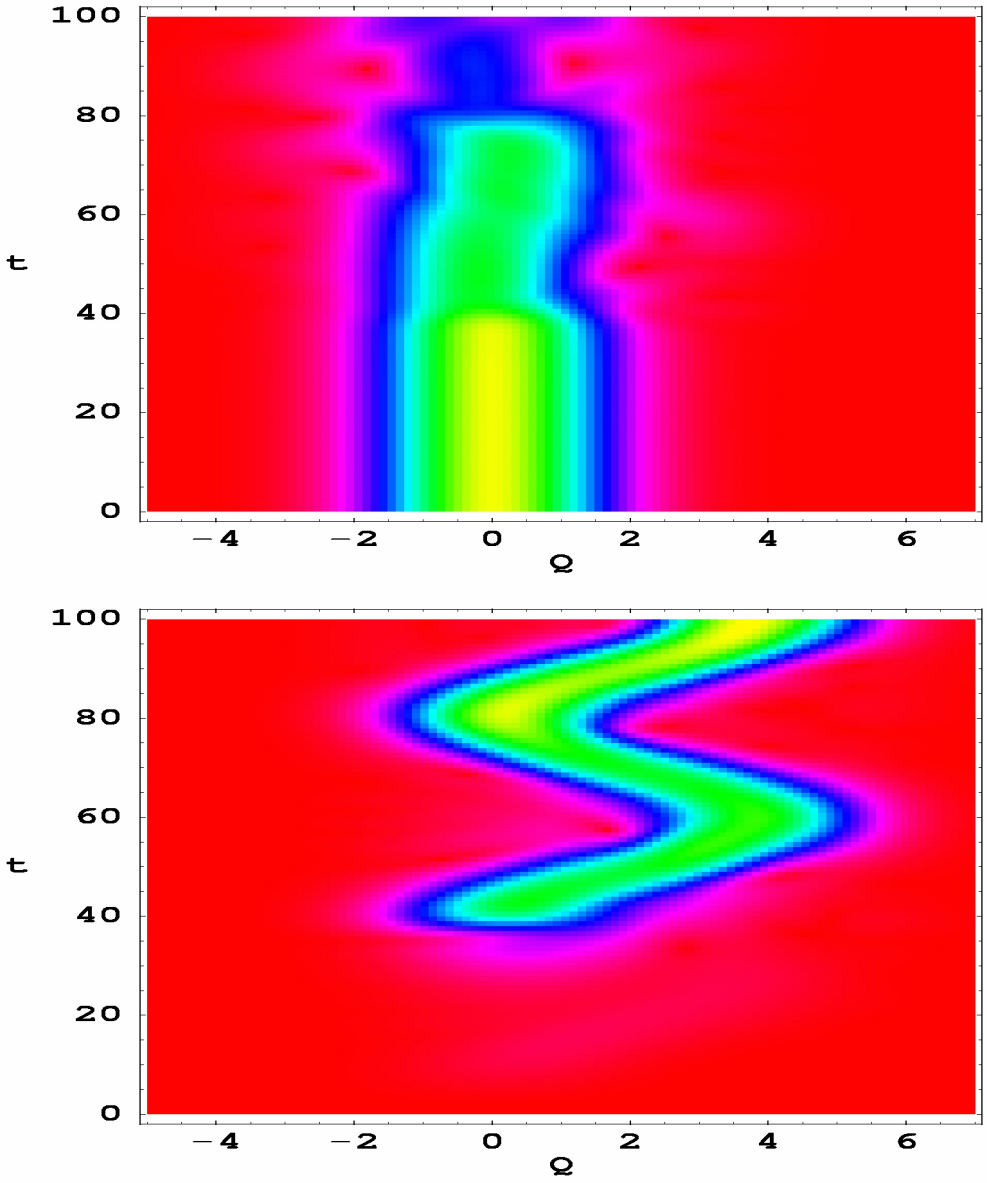

Vibrational wavepacket, ground state (upper panel),
excited state (lower panel).

- Control yield

$$J_0^{(20)} = |\langle \psi_{\text{tar}} | \psi^{(20)}(t_f) \rangle|^2 = 0.92.$$

Optimal Control Theory

Control functional

$$J[\mathbf{E}_c] = \mathcal{O}[\mathbf{E}_c] - \lambda(\frac{1}{2}\int_{t_0}^{t_f} dt\ \mathbf{E}_c^2(t) - I_0)$$

Functional equation determining the optimal pulse

$$\mathbf{E}_c(t) = \lambda \frac{\delta \mathcal{O}[\mathbf{E}_c]}{\delta \mathbf{E}_c(t)}$$

SOLUTION OF THE CONTROL PROBLEM

Control Functional

$$J[\mathbf{E}_\mathrm{c}] = |\langle\Psi_\mathrm{tar}|\Psi(t_f;\mathbf{E}_\mathrm{c})\rangle|^2 - \frac{\lambda}{2}\int_{t_0}^{t_f} dt\ \mathbf{E}_\mathrm{c}^2(t)$$

Self–Consistency Equation for the Optimal Field

$$\mathbf{E}_\mathrm{c}(t) = \frac{i}{\hbar\lambda}(\langle\Psi(t_f;\mathbf{E})_\mathrm{tar}|\Psi_\mathrm{c}\rangle\ \langle\Psi_\mathrm{tar}|U(t_f,t;\mathbf{E}_\mathrm{c})\ \hat{\mu}\ U(t,t_0;\mathbf{E}_\mathrm{c})|\Psi(t_0)\rangle + \mathrm{c.c.})$$

Coupled Forward–Backward Propagation

$$i\hbar\frac{\partial}{\partial t}|\Psi(t)\rangle = (H_\mathrm{mol} - \mathbf{E}_\mathrm{c}(t)\hat{\mu})|\Psi(t)\rangle$$

$$i\hbar\frac{\partial}{\partial t}|\Theta(t)\rangle = (H_\mathrm{mol} - \mathbf{E}_\mathrm{c}(t)\hat{\mu})|\Theta(t)\rangle$$

FIRST EXAMPLE

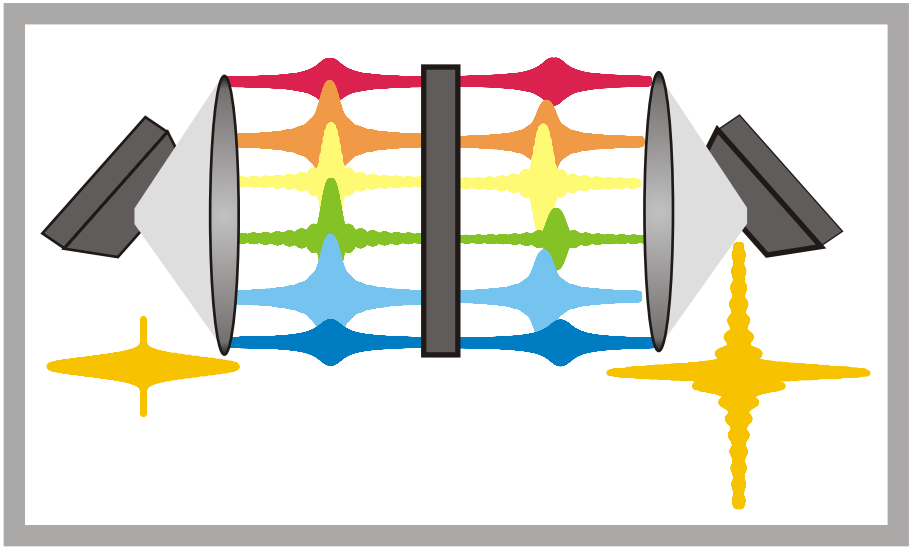

Complexity of the Control Task

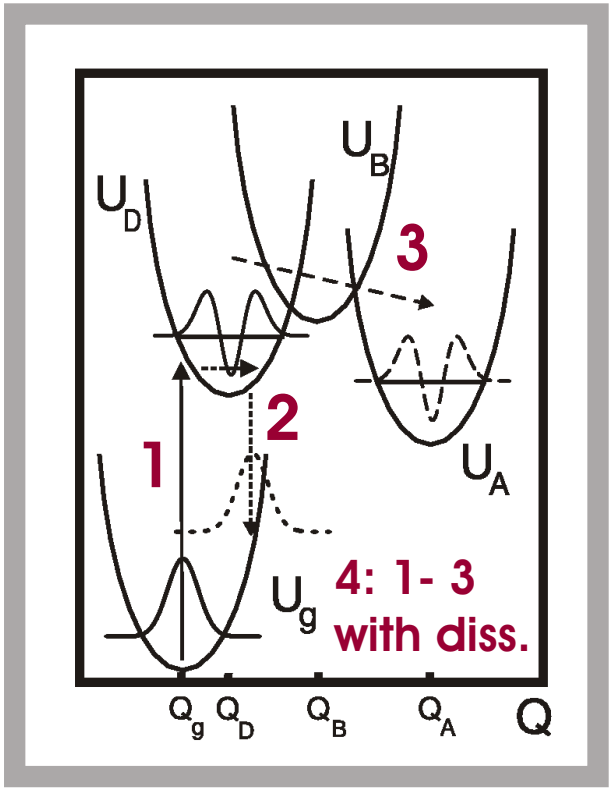

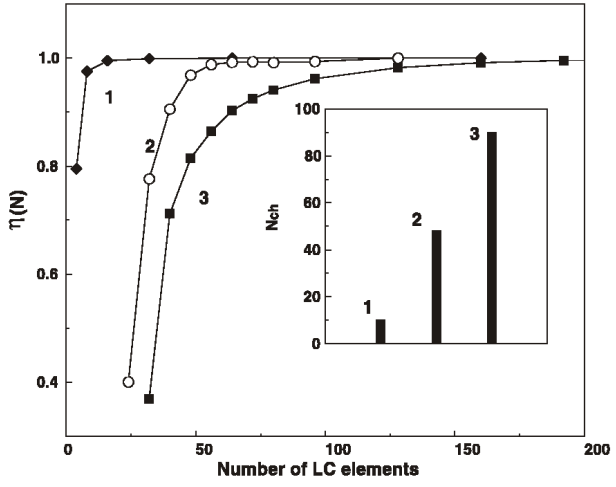

Fig. 3. The efficiency of the pulse shaper characterized by the ratio η versus the number N of liquid crystal cells in the shaper for the different control tasks of Fig. 1. Inset: N_{ch} leading to a 95% yield ordered with respect to the different control tasks.

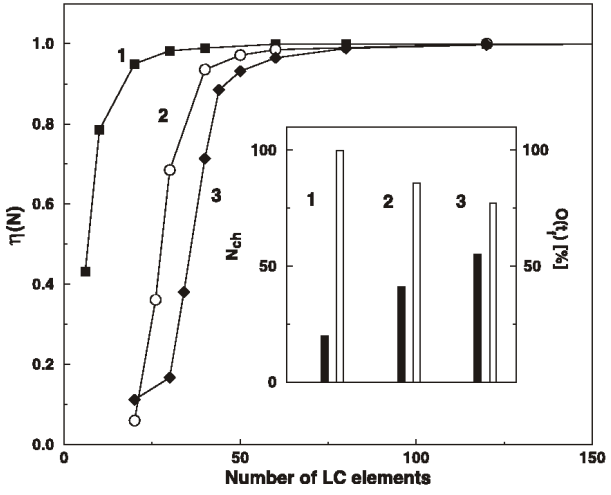

Fig. 4. The efficiency of the pulse shaper as shown in Fig. 3, but for the control task 4, and with different strength of dissipation. The vibrational life-time of the target level τ_t is used to characterize the strength of dissipation. 1. Without dissipation, 2. $\tau_t = 320$ fs, 3. $\tau_t = 640$ fs. Inset: N_{ch} as in Fig. 3 (black bar) and the population of the target state in percentage (white bar).

T. Mancal and V. M., CPL 362, 407 (2002)

SECOND EXAMPLE

Optimal Control Theory for Non-Resonant Multi-Photon Transitions

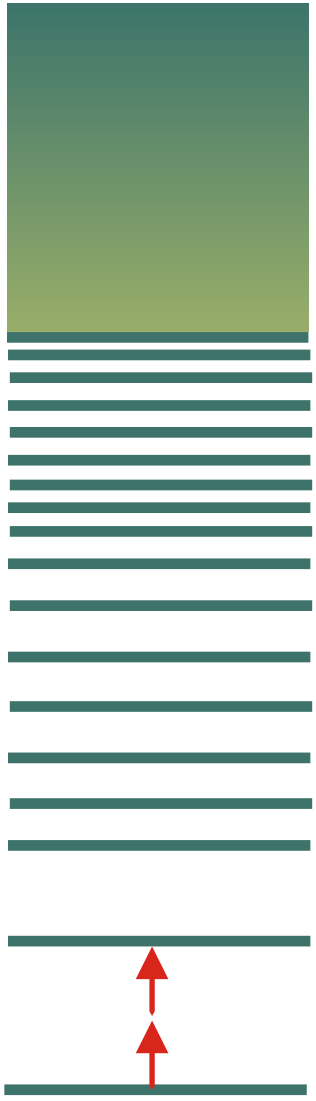

Standard scheme of OCT
using a target operator

$$\mathcal{O}[\mathbf{E}_c] = \langle \Psi(t;\mathbf{E}_c)|\hat{O}|\Psi(t;\mathbf{E}_c)\rangle$$

Non-Resonant Two-Photon Transitions

The RWA and the SVA

Coupled Schrödinger-equations for the vibrational wave functions

$$i\hbar\frac{\partial}{\partial t}|\chi_g(0;t)\rangle = (H_g - \frac{1}{2}|E(t)|^2 d_{gg}^{(\mathrm{II})})|\chi_g(0;t)\rangle - \frac{1}{4}E^{*2}(t)d_{ge}^{(\mathrm{II})}|\chi_e(2;t)\rangle$$

$$i\hbar\frac{\partial}{\partial t}|\chi_e(2;t)\rangle = (H_e - 2\hbar\omega_0 - \frac{1}{2}|E(t)|^2 d_{ee}^{(\mathrm{II})})|\chi_e(2;t)\rangle - \frac{1}{4}E^{2}(t)d_{eg}^{(\mathrm{II})}|\chi_g(0;t)\rangle$$

Control Functional

$$J(t_f;E,E^*) = |\ \langle\chi_e^{(\mathrm{tar})}|\chi_e(t_f)\rangle\ |^2 - \frac{\lambda}{4}\int_{t_0}^{t_f} dt\ |E(t)|^4$$

D. Ambrosek, M. Oppel, L. Gonzalez and V. M., special issue, Opt. Comm. 264, 502 (2006).

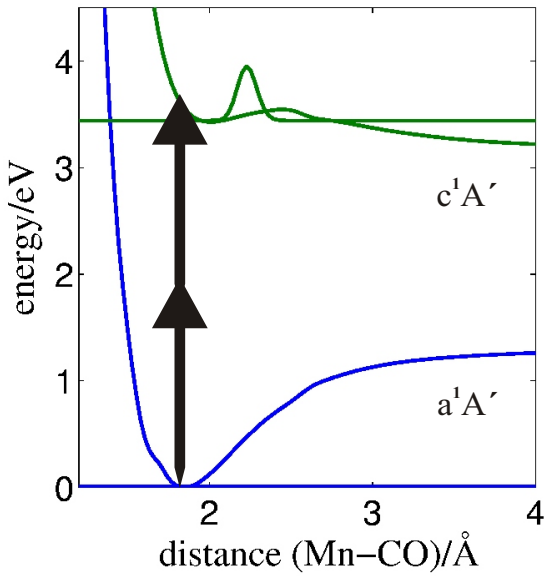

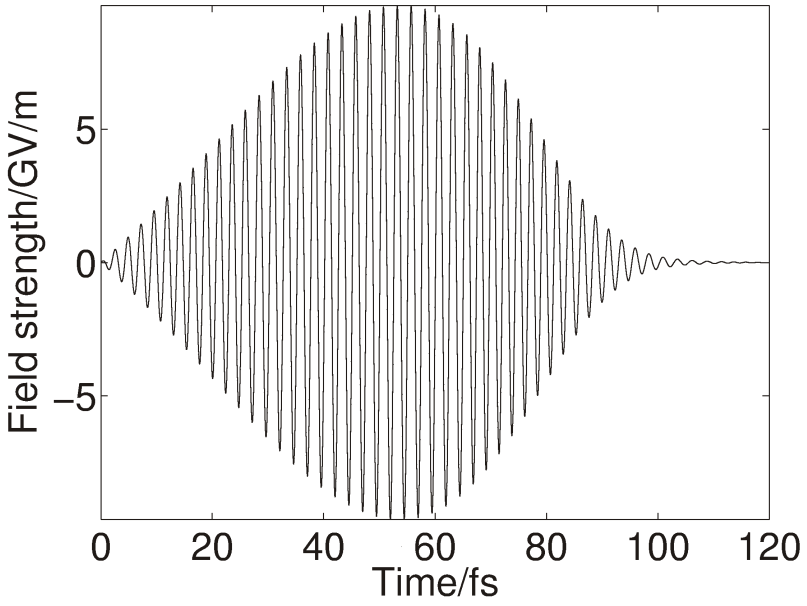

TABLE I: The yield $\mathcal{Q}$, the renormalized yield q, the maximum $E_{\max}$ of the field–strength (in GV/m) and the related intensity $I_{\max}$ (in GW/cm^2) for different used penalty factors λ (in 10^{12} fs (GV/m)^4) of the described control scheme

$\mathcal{Q}$	q	$E_{\max}$	$I_{\max}$	λ
0.68	0.82	58.1	3.02	3
0.29	0.74	42.2	2.19	12
0.0049	0.72	14.7	0.76	19
0.0009	0.72	9.6	0.50	20

THIRD EXAMPLE

OCT with a target operator distributed in time and parameter space

$$\mathcal{O}[\mathbf{E}_c] = \int_{t_0}^{\infty} dt \int dp \, \langle \Psi(t;p) | \hat{O}(t;p) | \Psi(t;p) \rangle$$

Shi, Rabitz, JCP 92, 364 (1990), 97, 276 (1992)

direct optimization of transient probe pulse absorption in a pump-probe scheme
A. Kaiser, and V. M., JCP 121, 2528 (2004), CPL 405, 339 (2005), CP 320, 95 (2006)
consideration of structural and energetic disorder

Direct Optimization of a Probe-Pulse Transient Absorption

Three level scheme for NaK

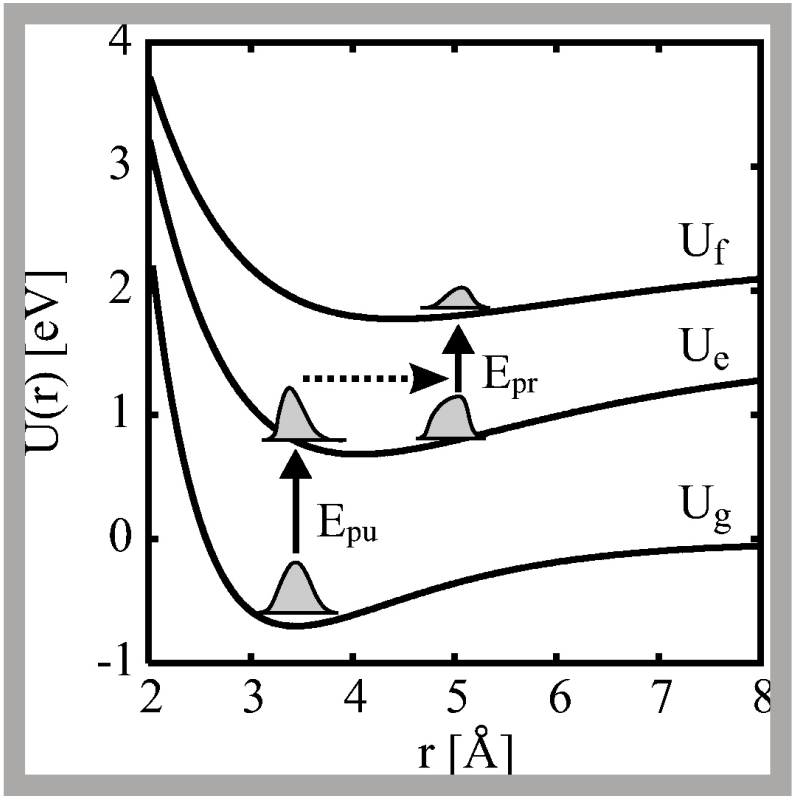

$1^1\ ^{1+}$ - ground-state
$2^1\ ^{1+}$ - first-excited states
$3^1\ ^{+}$ - higher excited state

probe pulse
transient absorption signal

$$S_{\mathrm{pr}} = -\int dt\, \frac{\partial \mathbf{E}_{\mathrm{pr}}(t)}{\partial t} \mathbf{P}_{\mathrm{pr}}(t; \mathbf{E}_{\mathrm{c}})$$

$$\mathbf{P}_{\mathrm{pr}}(t) = n_{\mathrm{mol}} \langle \Psi(t; \mathbf{E}_{\mathrm{c}}, \mathbf{E}_{\mathrm{pr}}) | \hat{\mu} | \Psi(t; \mathbf{E}_{\mathrm{c}}, \mathbf{E}_{\mathrm{pr}}) \rangle - n_{\mathrm{mol}} \langle \Psi(t; \mathbf{E}_{\mathrm{c}}) | \hat{\mu} | \Psi(t; \mathbf{E}_{\mathrm{c}}) \rangle$$

probe pulse
polarization

Optimized Probe Pulse Transient Absorption Signal versus Probe Pulse Length

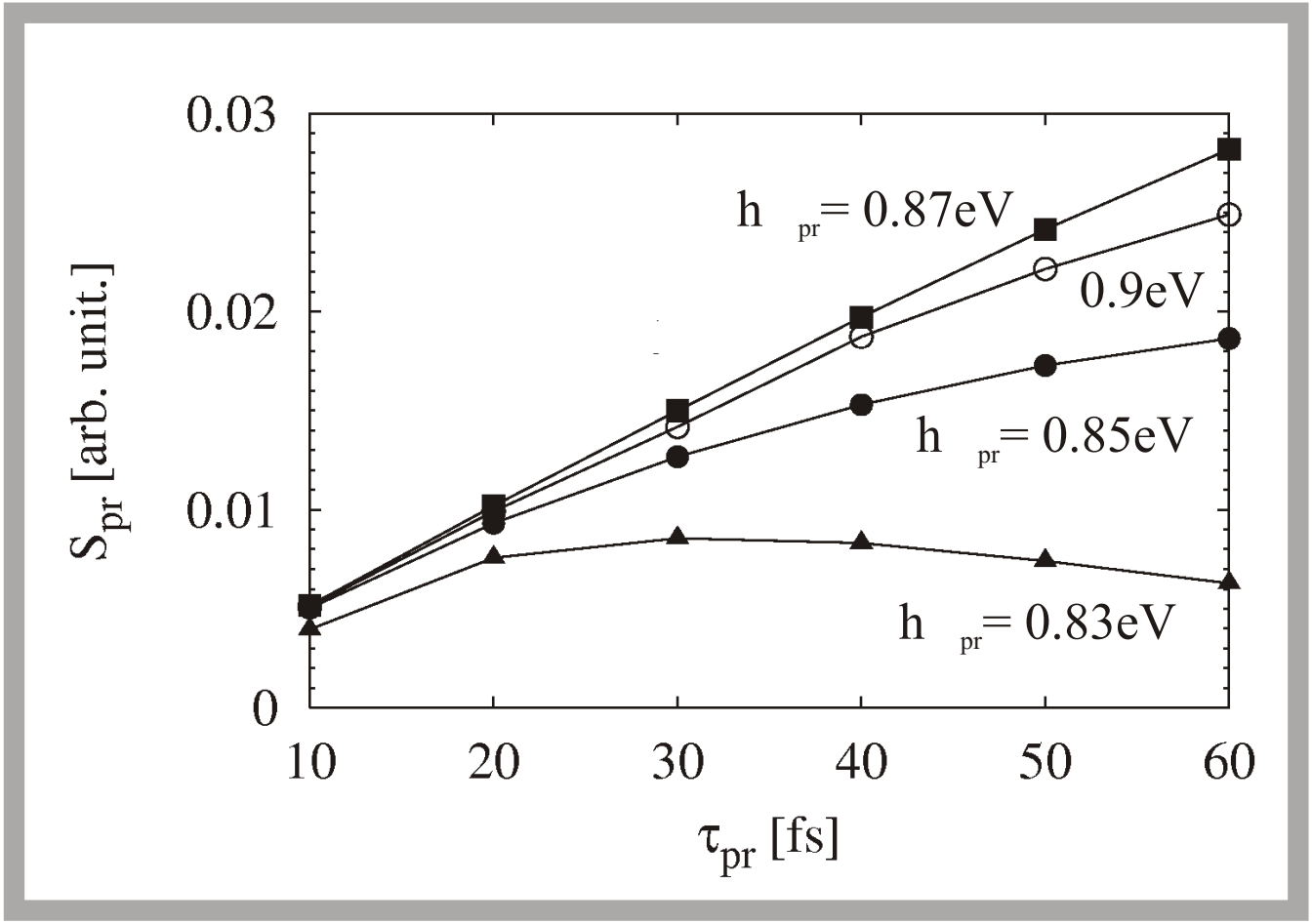

-> control pulse acts up to 1.5 ps

-> probe pulse is centered at 1.6 ps

A. Kaiser, and V. M., JCP 121, 2528 (2004), CPL 405, 339 (2005), CP (2005)

FOURTH EXAMPLE

OCT for open system dynamics

$$\mathcal{O}[\mathbf{E}_c] = \mathrm{tr}\{\hat{\rho}(t_f;\mathbf{E}_c)\hat{O}\}$$

$$\mathbf{E}_c(t) = \frac{i}{\hbar\lambda}\mathrm{tr}\{\hat{O}\mathcal{U}(t_f,t;\mathbf{E}_c)\,[\hat{\mu},\hat{\rho}(t;\mathbf{E}_c)]_-\}$$

Bartana, Kosloff, Tannor, JCP 106, 1435 (1997)
Ohtsuki, Yhu, Rabitz, JCP 110, 9825 (1999)
Mancal, Kleinekathöfer, May, JCP 117, 636 (2002)
Xu, Yan, Ohtsuki, Fujimura, Rabitz, JCP 120, 6600 (2004)
Brüggemannm, May, JPCB 108, 10529 (2004)

Excitation Energy Localization in a Pigment Protein Complex

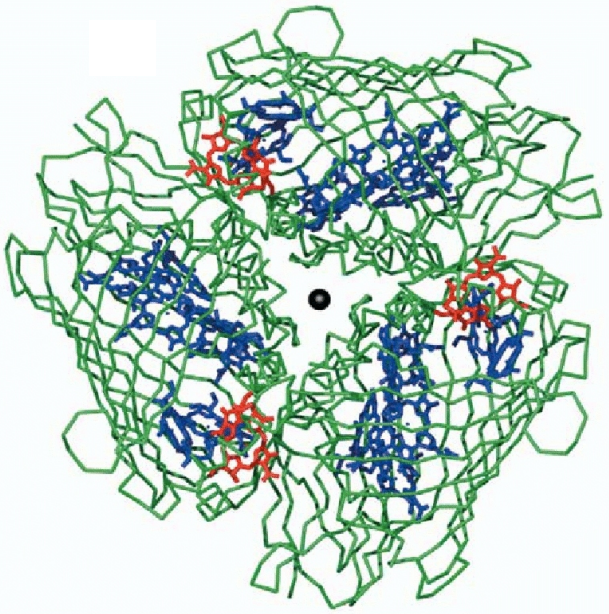

$$\mathcal{O}[\mathbf{E}_c] = \mathrm{tr}\{\hat{\rho}(t;\mathbf{E}_c)\hat{O}\}$$

$$\mathcal{O}[\mathbf{E}_c] = \int_{t_0}^{\infty} dt \int dp \, \langle \Psi(t;p)|\hat{O}(t;p)|\Psi(t;p)\rangle$$

Excitation Energy Localization via the Formation of Excitonic Wavepackets

Vibrational Wavepackets versus Excitonic Wavepackets

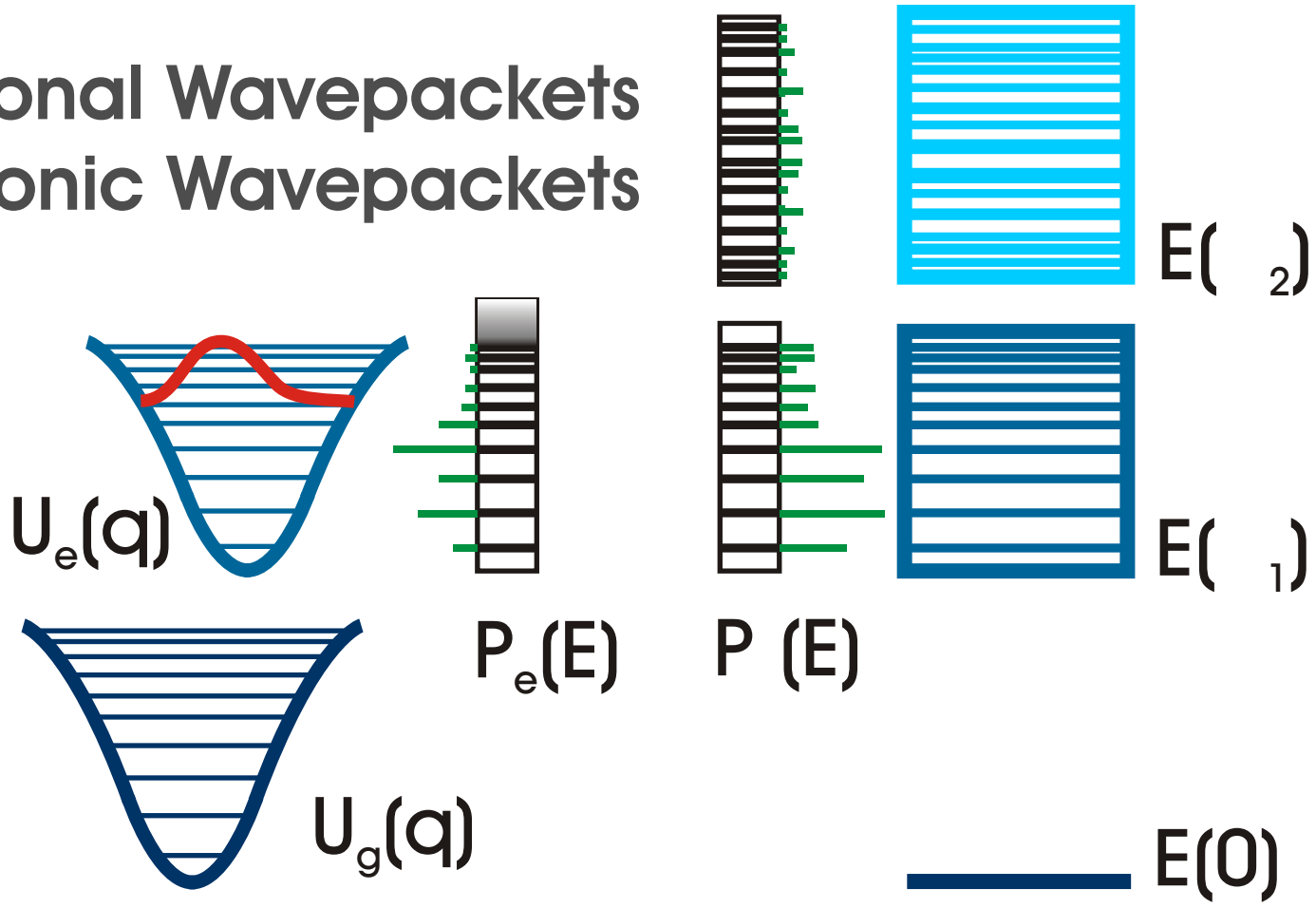

The study of particular relaxation pathways may become possible!

Simulating femtosecond dynamics of excitons in chromophore complexes:

- formation of single- and two-exciton states
- electronic excitation energy dissipation
- presence of static disorder

ab initio description of the single-exciton states possible (Schulten, 1998, ...)

description of all other effects requires the introduction of certain models

Electronic Level Scheme

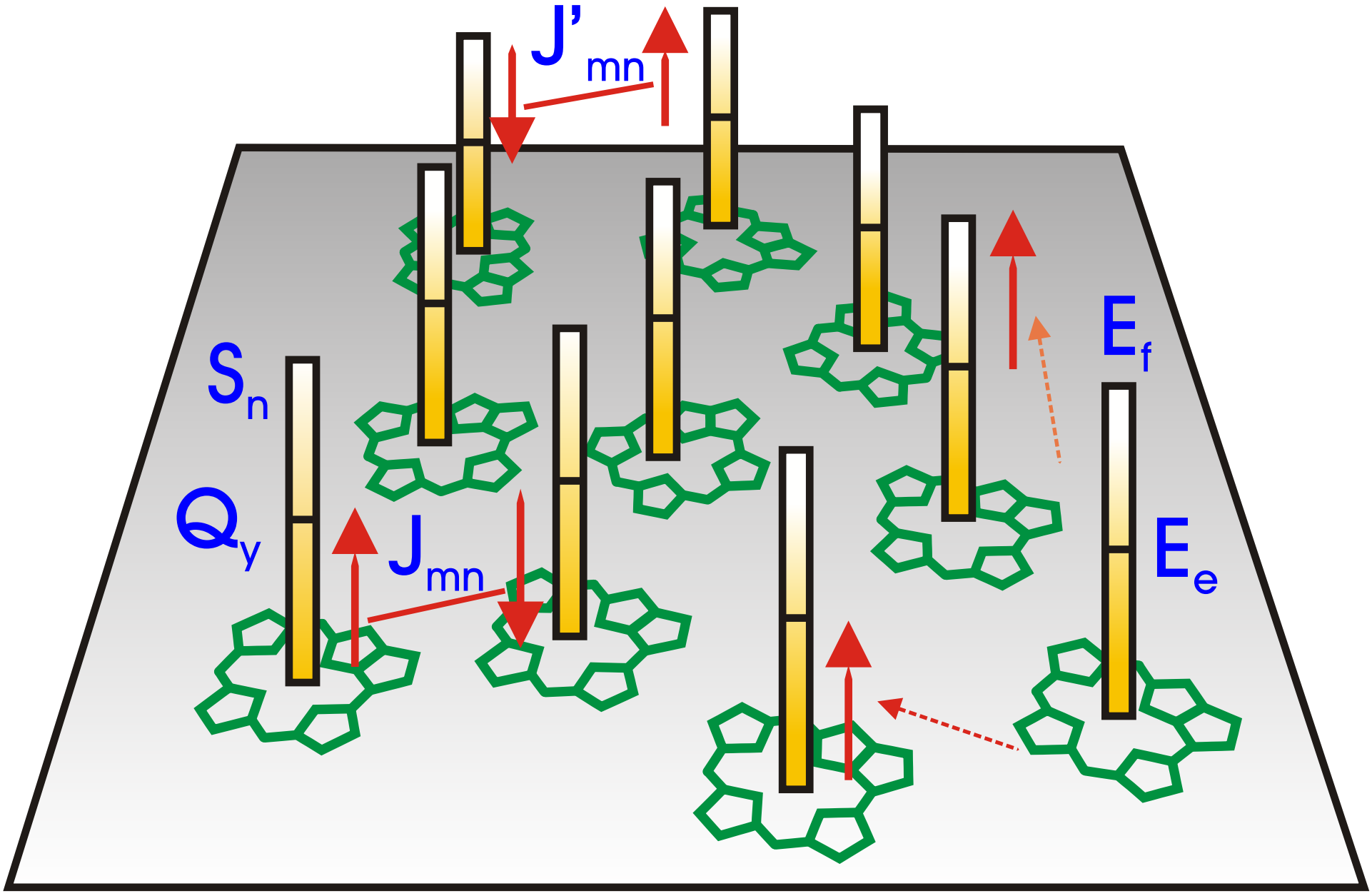

Formation of Delocalized Single- and Two-Exciton States

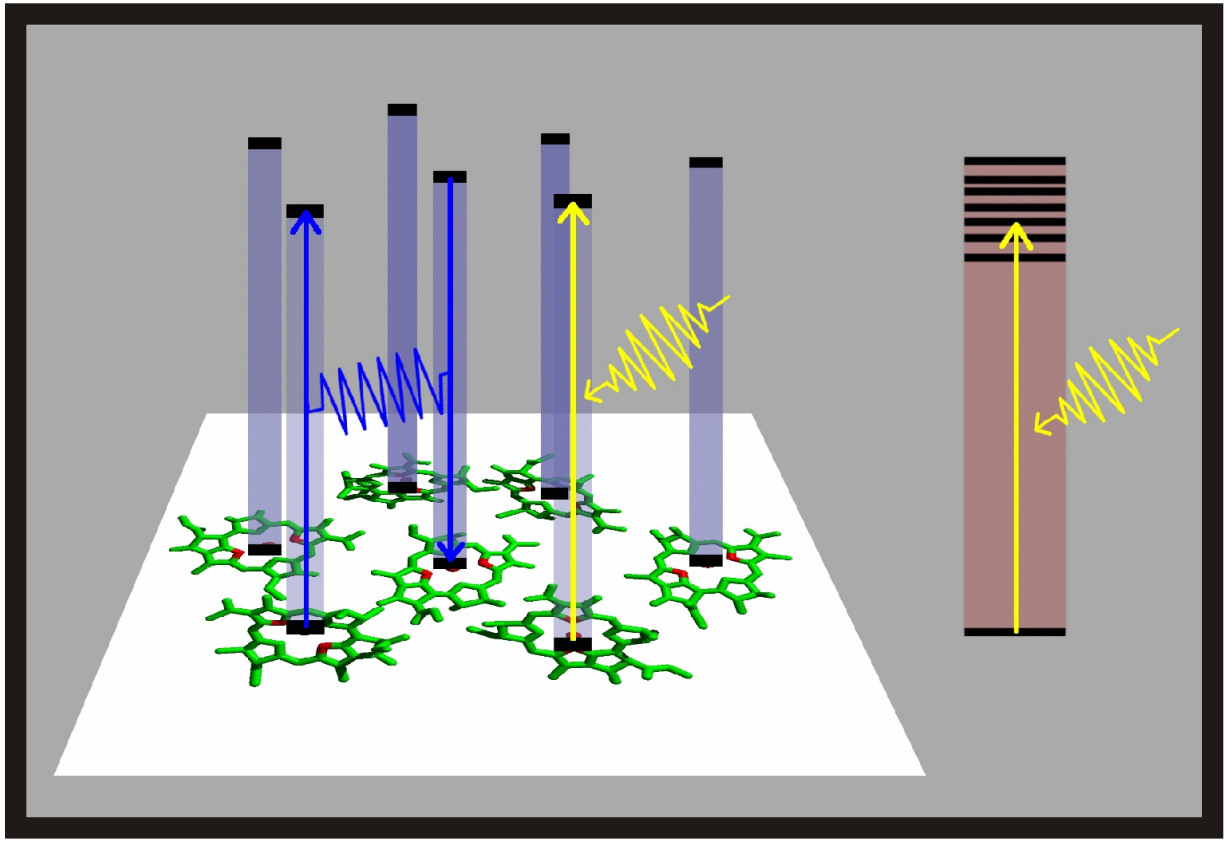

ground-state

$$|\alpha_0\rangle = \prod_m |\varphi_{mg}\rangle$$

single exciton state

$$|\alpha_1\rangle = \sum_m C(\alpha_1; m)|\phi_m\rangle$$

two-exciton state

$$|\alpha_2\rangle = \sum_{m,n} C(\alpha_2; mn)|\phi_{mn}\rangle$$

Th. Renger, V. M., and O. Kühn,
Phys. Rep. 343, 137 (2001)

Excitonic Wavepacket

$$|\alpha\rangle = \sum_m C_\alpha(m)|\phi_m\rangle \quad \Longrightarrow \quad |\phi_{m_{\rm tar}}\rangle = \sum_\alpha C^*_\alpha(m_{\rm tar})|\alpha\rangle$$

Linear response expression for the driven wave function

$$|\phi_{m_{\rm tar}}\rangle = |\Psi(t_f)\rangle \approx \frac{i}{\hbar}\sum_\alpha \int_{t_0}^{t_f} d\bar{t}\; e^{-i\Omega_\alpha(t-\bar{t})}\mathbf{d}_\alpha\mathbf{E}(\bar{t})|\alpha\rangle \approx \frac{i}{\hbar}\sum_\alpha e^{-i\Omega_\alpha t}\mathbf{d}_\alpha\mathbf{E}(\Omega_\alpha)|\alpha\rangle$$

Estimate of the Control Field

$$\mathbf{E}(t) \approx -i\hbar\sqrt{\mathcal{N}}\, f(t)\mathbf{e}\sum_\alpha e^{-i\Omega_\alpha(t-t_f)}\frac{C^*_\alpha(m_{\rm tar})}{d_\alpha} + \text{c.c.}$$

Optimization of the target chromophor population

$$P_{m_{\mathrm{tar}}}(t_f) = \frac{1}{N_{\mathrm{CC}}} \sum_p \sum_{\alpha,\beta} C_p(\alpha; m_{\mathrm{tar}}) C_p^*(\beta; m_{\mathrm{tar}}) \rho_p(\alpha, \beta; t_f)$$

$$\rho(\alpha_M, \beta_N; t) = \langle \alpha_M | \hat{\rho}(t) | \beta_N \rangle$$

multiexciton density operator

multiexciton Quantum Master Equation

$$\frac{\partial}{\partial t}\hat{\rho}(t) = -\frac{i}{\hbar}[H_{\mathrm{mx}} + H_{\mathrm{field}}(t), \hat{\rho}(t)] - (\mathcal{R}_{\mathrm{mx-vib}} + \mathcal{R}_{\mathrm{eea}})\hat{\rho}(t)$$

external field induced coherent motion

exciton relaxation

exciton-exciton annihilation

Monomeric Structure of the FMO Complex and Distribution of Exciton Expansion Coefficients

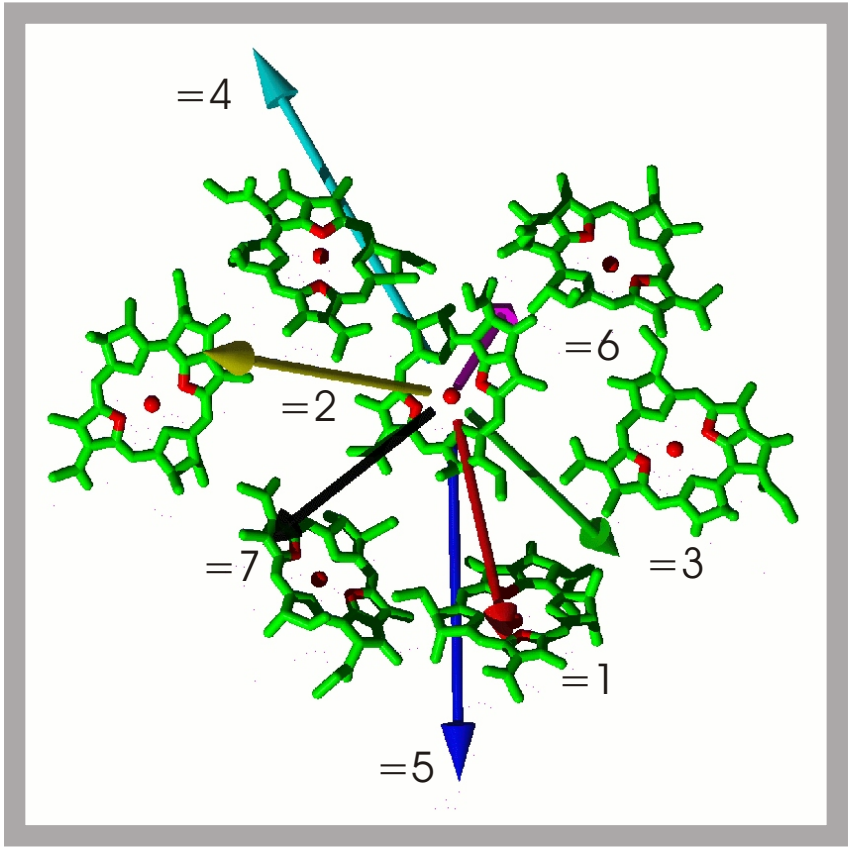

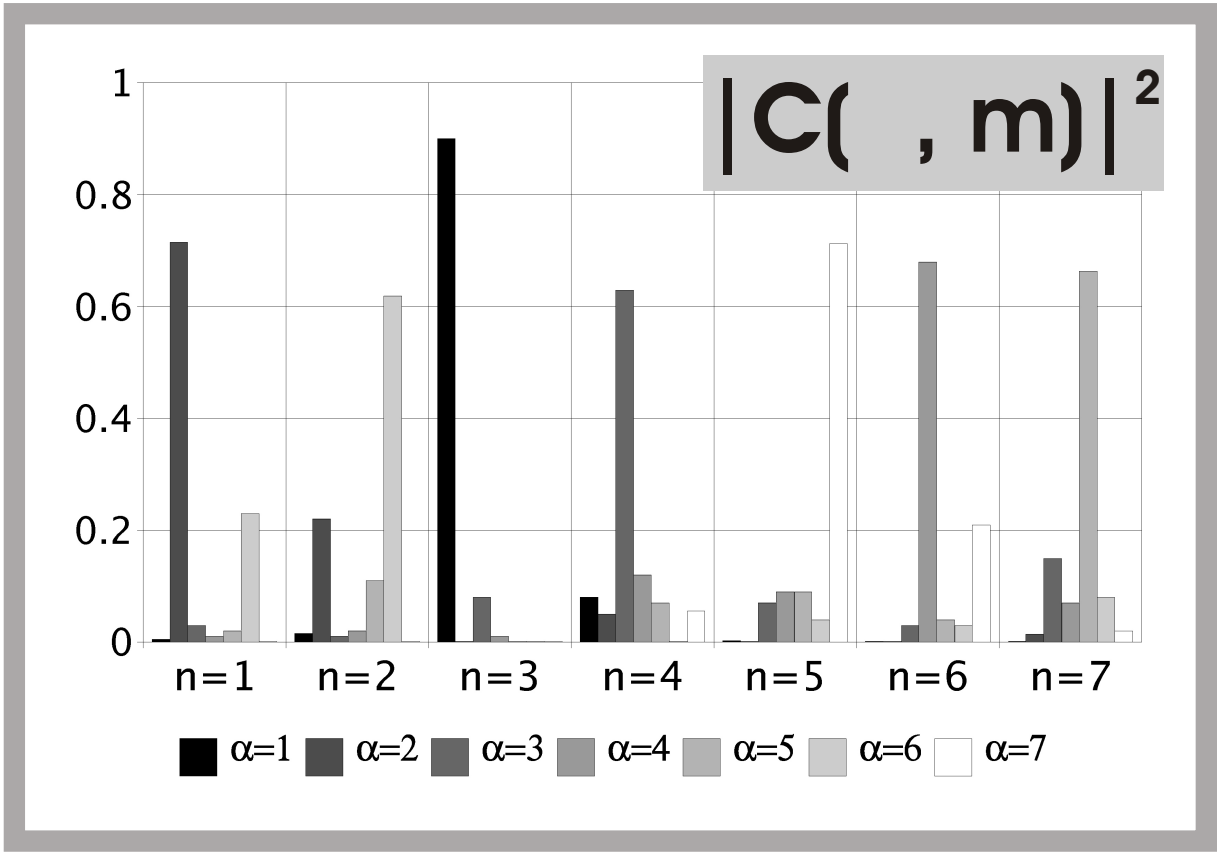

Laser Pulse Excitation Energy Localization in the FMO-Complex

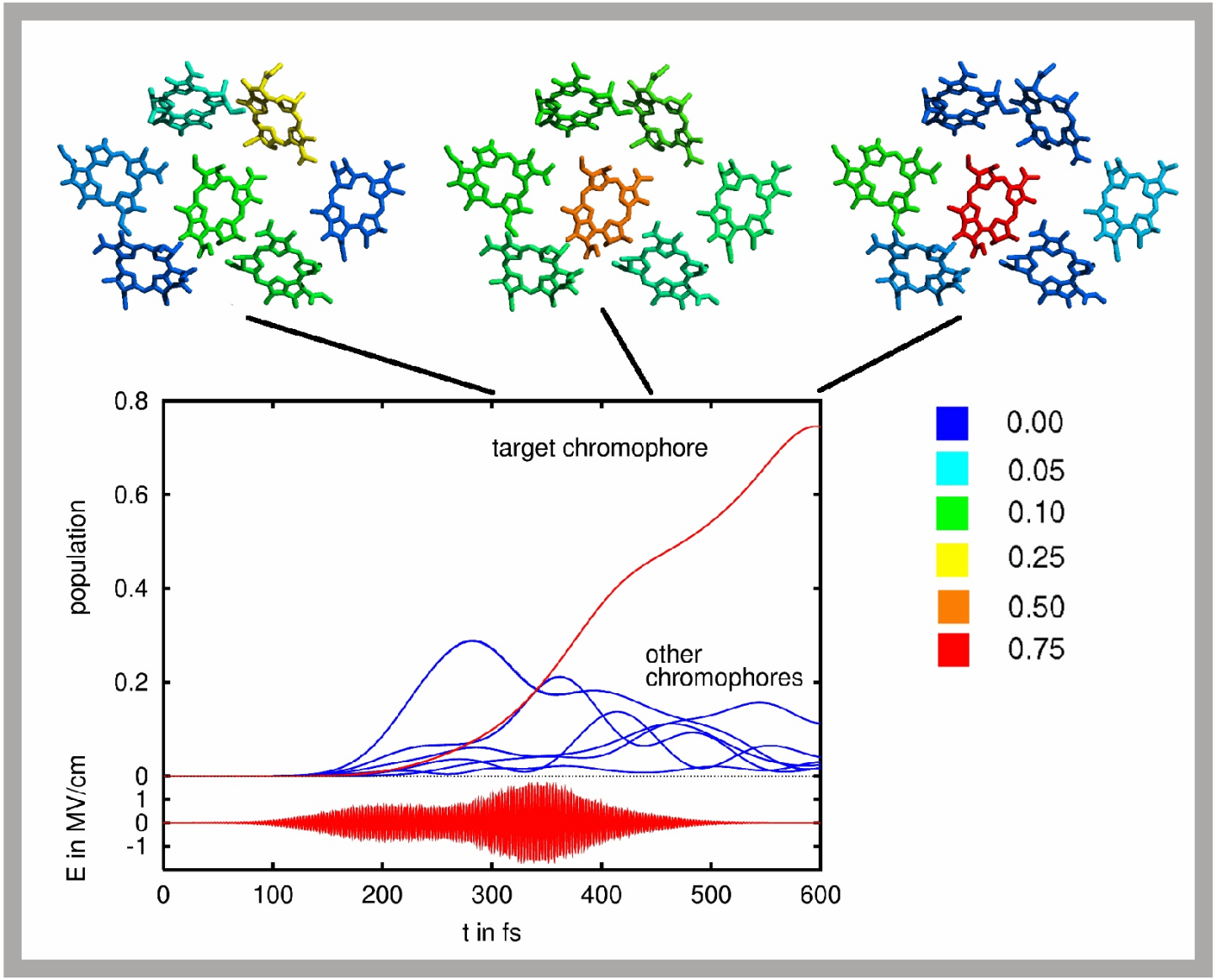

B. Brüggemann, and V. M., JPC B 108, 10529 (2004)

Excitation Energy Localization at Chromophore m=7

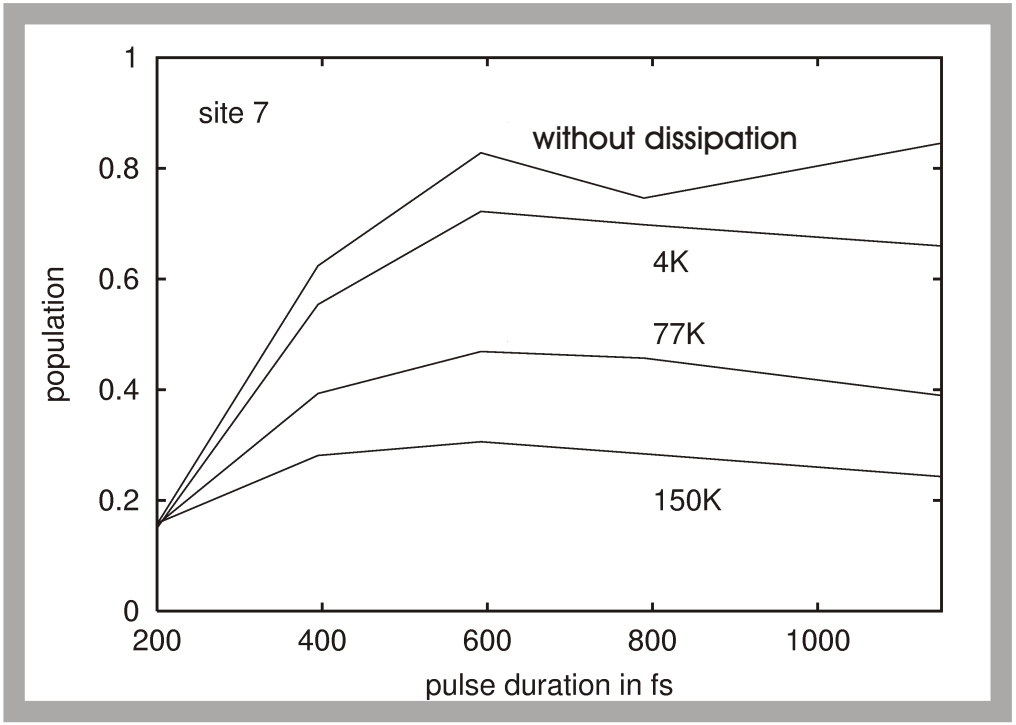

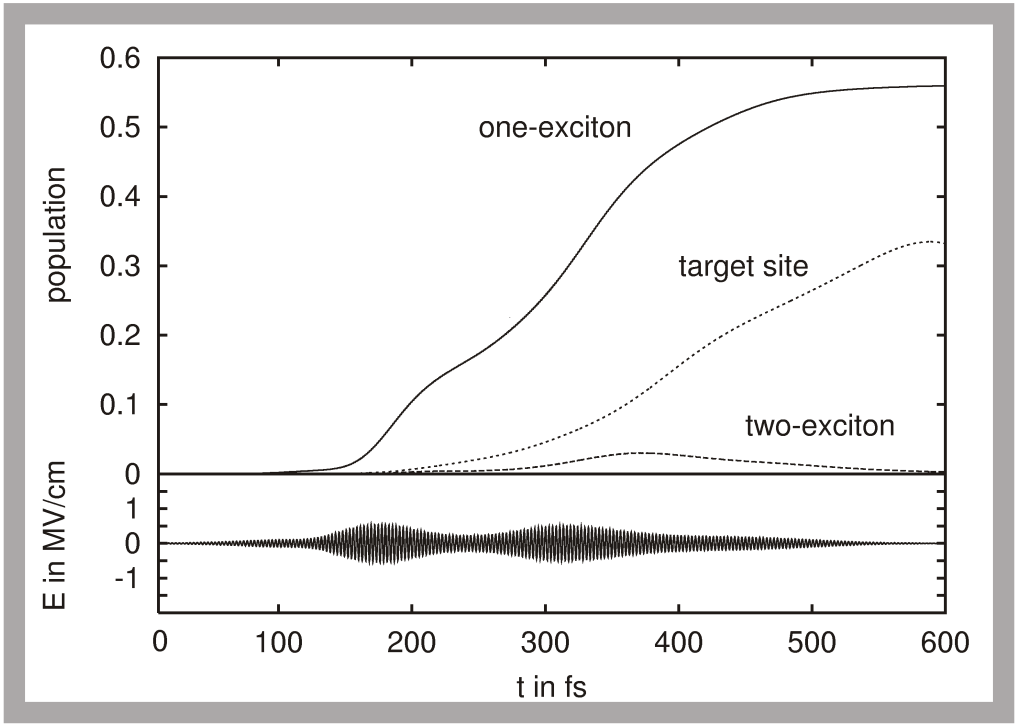

in dependence on
- the control pulse length
- temperture

- including two-exciton states
- at a temperature of 4 K

Polarization Shaping

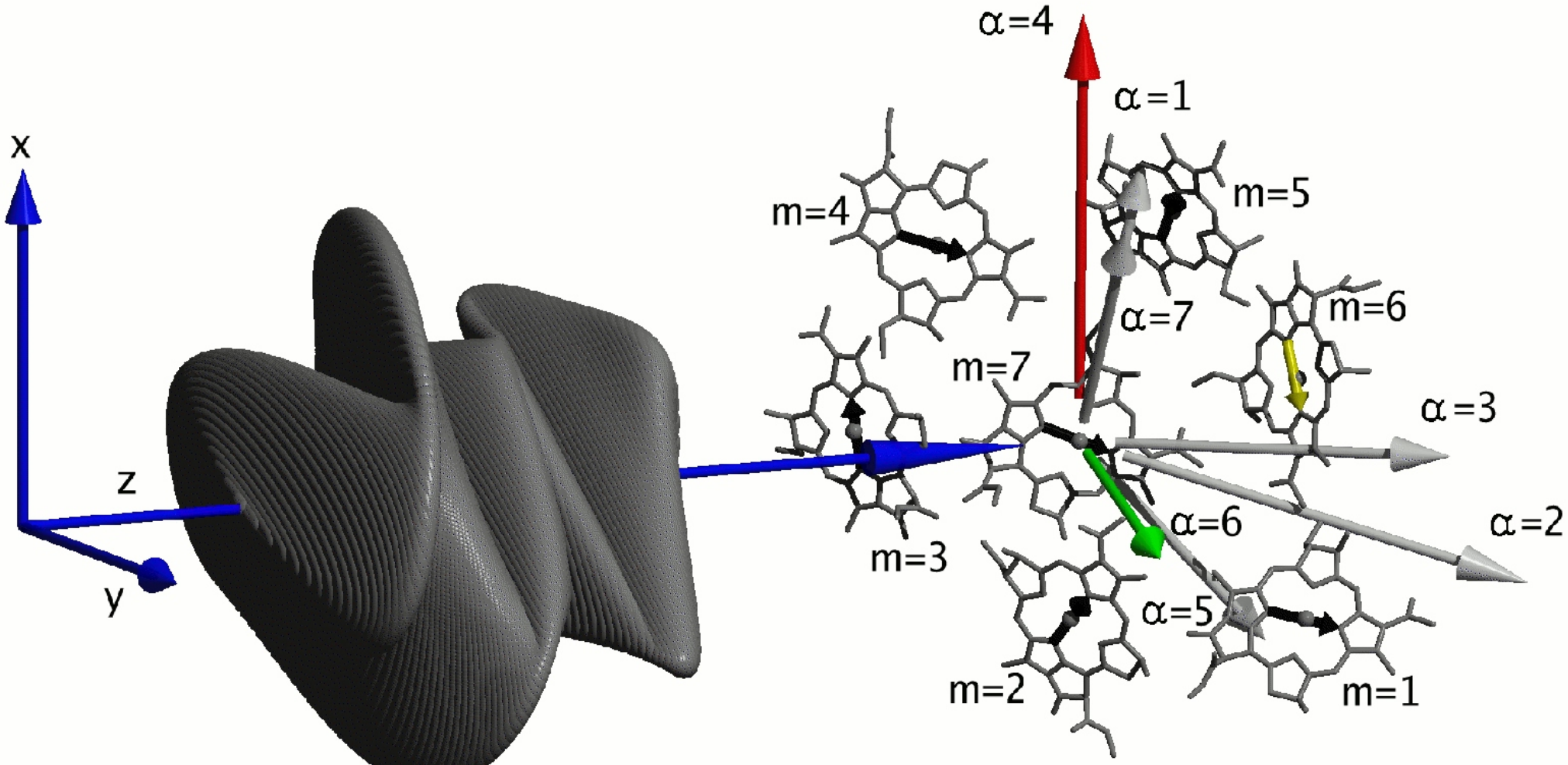

Linear versus circular polarization of the control pulse

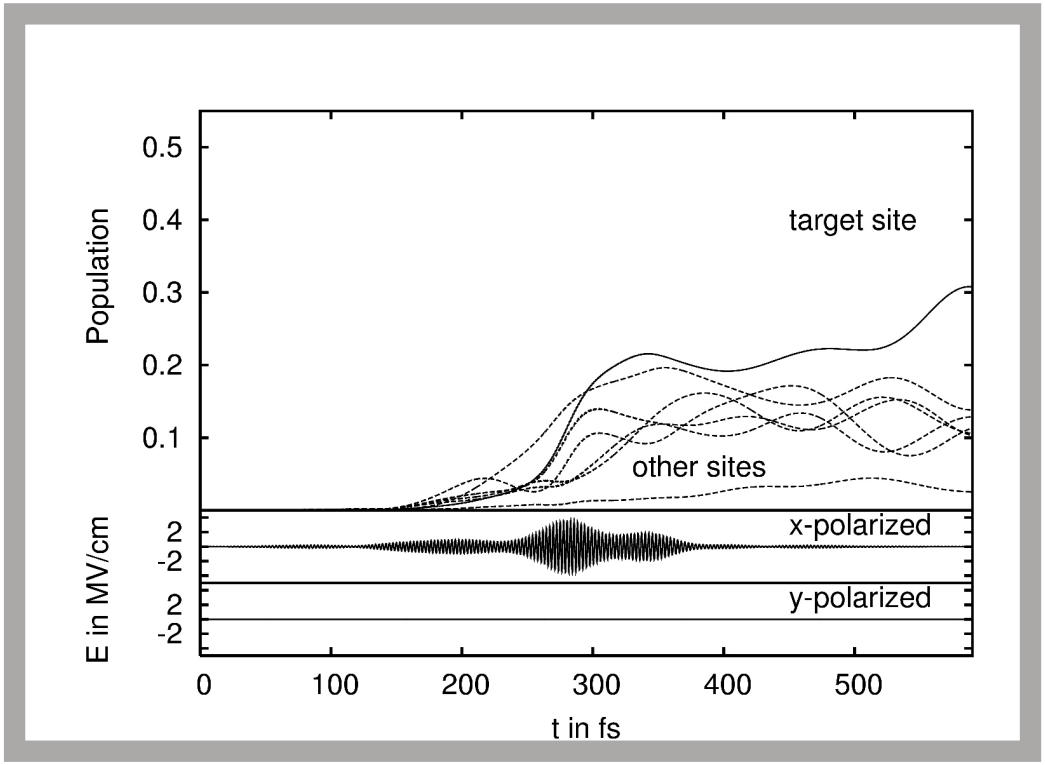

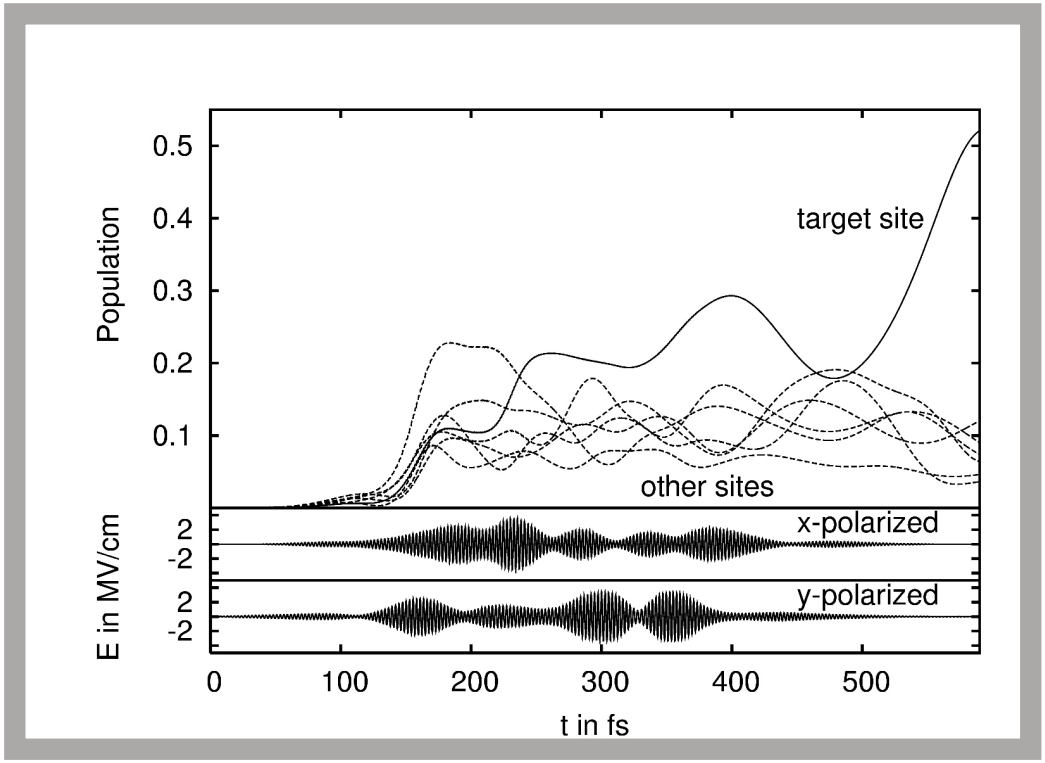

-> 10 randomly oriented complexes, -> energetic disorder of 100 cm^{-1},
-> 4 K, -> neglect of two-exciton levels,

self-consistency equation for the components of the optimal field

$$E_{j=x,y}(t) = \frac{1}{N_{\mathrm{CC}}} \sum_p \frac{i}{\hbar\lambda} \mathrm{tr}_{\mathrm{mx}}\{\hat{\theta}_p(t; E_x, E_y)\,[\hat{\mu}_{pj=x,y}, \hat{\rho}_p(t; E_x, E_y)]_-\}$$

FIFTH EXAMPLE

Laser Pulse Control of Multimode Vibrational Dynamics in Pyrazine

$$\mathcal{O}[\mathbf{E}_c] = \langle \Psi(t;\mathbf{E}_c)|\hat{O}|\Psi(t;\mathbf{E}_c)\rangle$$

plus

Multi Configuration

Time-Dependent Hartree Method

4-Mode Model of Pyrazine (vibronic coupling model)

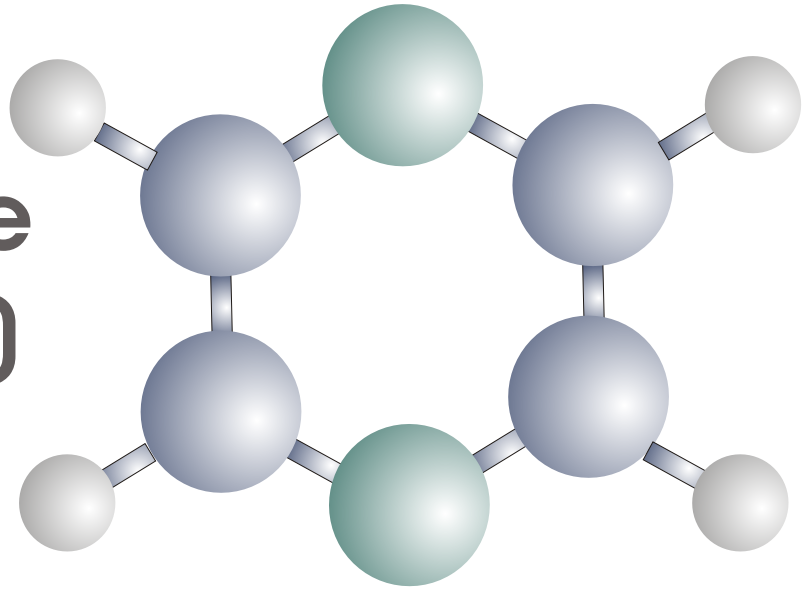

Worth, Meyer, and Cederbaum,
JCP 109, 3518 (1998)

tuning modes

coupling mode

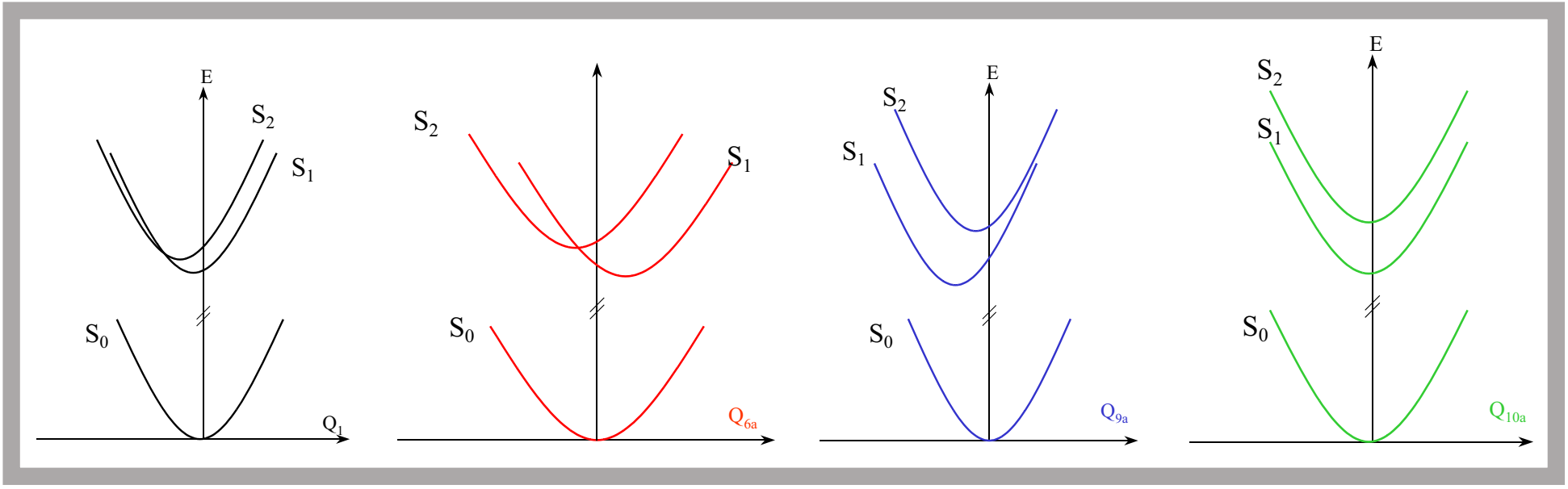

ring stretching

ring bending

out of plane

Optimization of the overall S_1-population

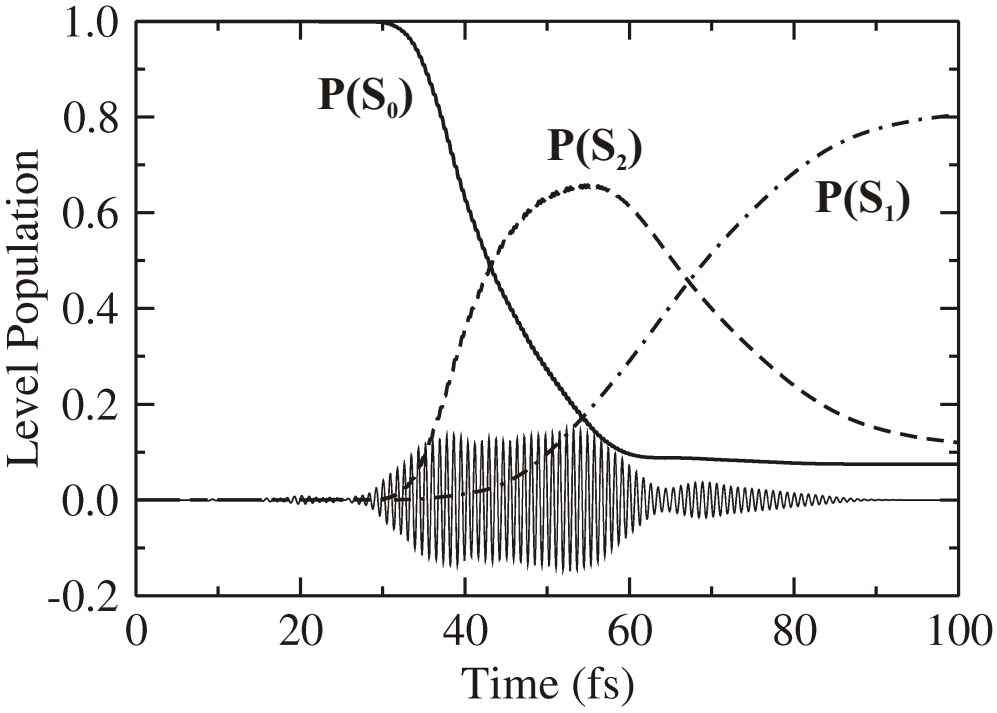

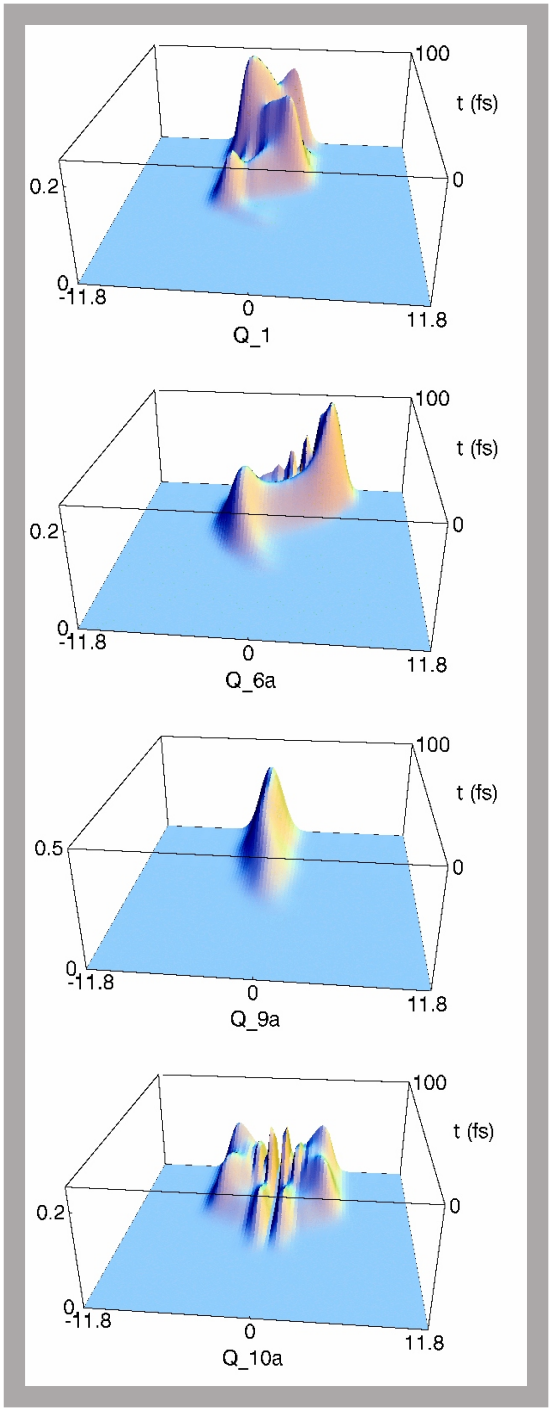

Reduced probability distribution of the four modes

$$P_{S_1}(Q_j, t) = \int dQ' \, |\chi_{S_1}(Q_1, Q_{6a}, Q_{9a}, Q_{10a}, t)|^2$$

L. Wang, H.-D. Meyer, and V. M., JCP 125, 014102 (2006)

OUTLOOK

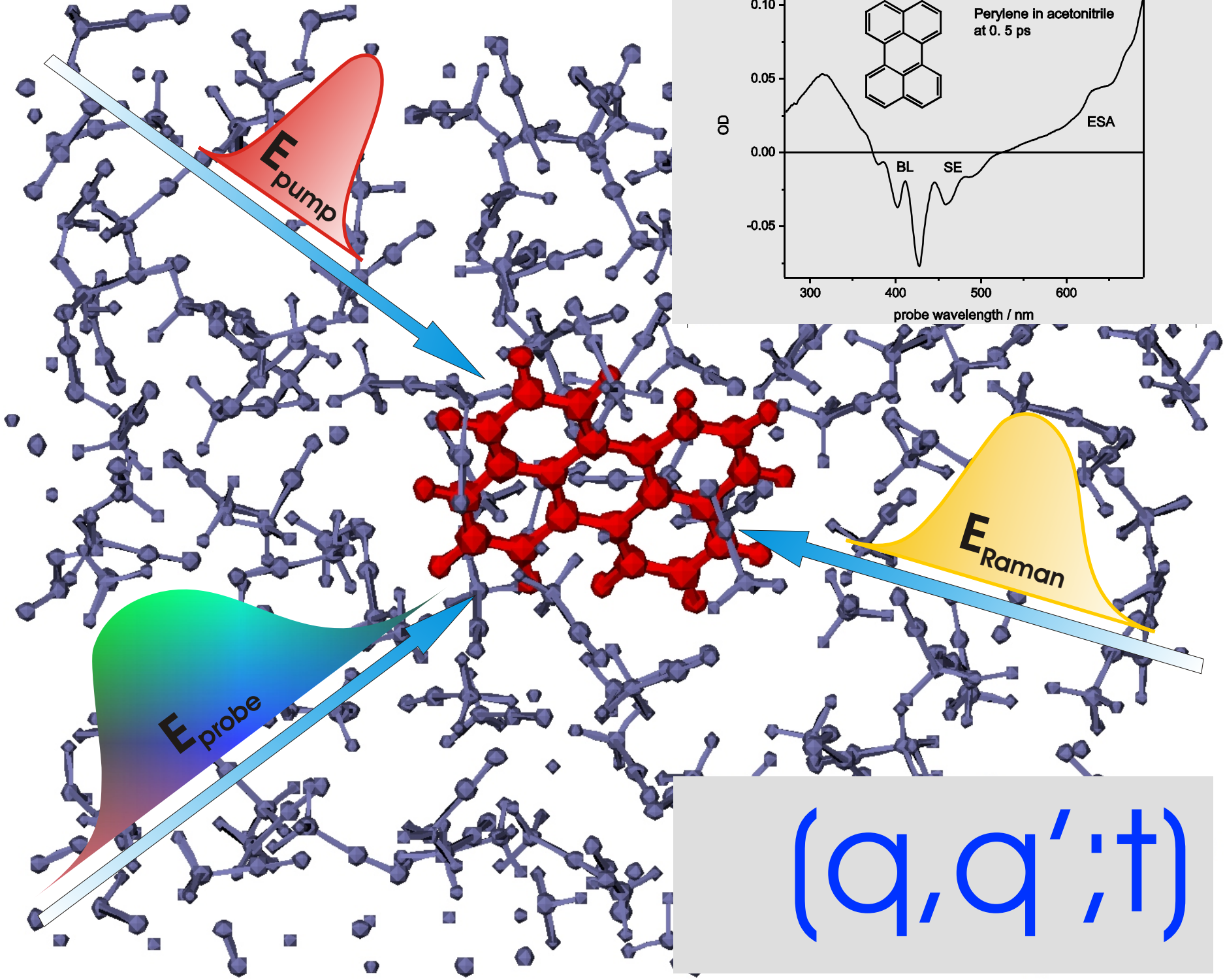
E pump
E probe
E Raman
Perylene in acetonitrile
at 0. 5 ps
0.10
0.05
0.00
-0.05
OD
BL
SE
ESA
300
400
500
600
probe wavelength / nm
(q,q';t)